

AD-A224 681

## REPORT DOCUMENTATION PAGE

Form Approved  
OMB No. 0704-0188

Public reporting burden for this collection of information is estimated to average 1 hour per response, including the time for reviewing instructions, searching existing data sources, gathering and maintaining the data needed, and completing and reviewing the collection of information. Send comments regarding this burden estimate or any other aspect of this collection of information, including suggestions for reducing this burden, to Washington Headquarters Services, Directorate for Information Operations and Reports, 1215 Jefferson Davis Highway, Suite 1204 Arlington, VA 22202-4302, and to the Office of Management and Budget, Paperwork Reduction Project (0704-0188), Washington, DC 20503.

1. AGENCY USE ONLY (Leave blank)

2. REPORT DATE

August 1990

3. REPORT TYPE AND DATES COVERED

~~THESIS~~ Dissertation

4. TITLE AND SUBTITLE

Studies of Thin Film Chemical Sensors Using the Quartz  
Crystal Microbalance

5. FUNDING NUMBERS

6. AUTHOR(S)

Howard R. Meyer, Jr.

7. PERFORMING ORGANIZATION NAME(S) AND ADDRESS(ES)

AFIT Student at: University of Wyoming

8. PERFORMING ORGANIZATION  
REPORT NUMBER

AFIT/CI/CIA -90-017D

9. SPONSORING/MONITORING AGENCY NAME(S) AND ADDRESS(ES)

AFIT/CI

Wright-Patterson AFB OH 45433

10. SPONSORING/MONITORING  
AGENCY REPORT NUMBER

11. SUPPLEMENTARY NOTES

12a. DISTRIBUTION / AVAILABILITY STATEMENT

Approved for Public Release IAW AFR 190-1  
Distribution Unlimited  
ERNEST A. HAYGOOD, 1st Lt, USAF  
Executive Officer, Civilian Institution Programs

12b. DISTRIBUTION CODE

13. ABSTRACT (Maximum 200 words)

DTIC  
ELECTE  
AUG 1 1990  
S B D

14. SUBJECT TERMS

15. NUMBER OF PAGES

108

16. PRICE CODE

17. SECURITY CLASSIFICATION  
OF REPORT

UNCLASSIFIED

18. SECURITY CLASSIFICATION  
OF THIS PAGE19. SECURITY CLASSIFICATION  
OF ABSTRACT

20. LIMITATION OF ABSTRACT

Studies of Thin Film Chemical Sensors Using the Quartz  
Crystal Microbalance

by

Howard R. Meyer, Jr.

A dissertation

submitted to

The Department of Chemistry and

The Graduate School of The University of Wyoming

in Partial Fulfillment of Requirements

for the Degree of

DOCTOR OF PHILOSOPHY

in

CHEMISTRY

Laramie, Wyoming

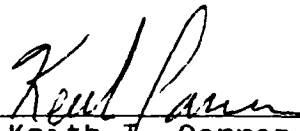
August, 1990

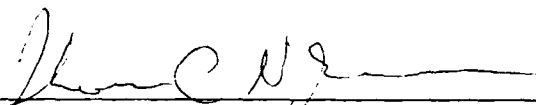
TO THE OFFICE OF THE GRADUATE SCHOOL:

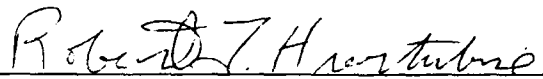
The members of the committee approve the dissertation  
of Howard R. Meyer, Jr., presented on June 27, 1990.

  
Dr. Daniel A. Buttry, Chairman

  
Dr. Vernon S. Archer

  
Dr. Keith T. Carron

  
Dr. Thomas C. Vogelmann

  
Dr. Robert J. Hurturbise

Accession For	
NTIS GRA&I	<input checked="checked" type="checkbox"/>
DTIC TAB	<input type="checkbox"/>
Unannounced	<input type="checkbox"/>
Justification	
By	
Distribution/	
Availability Codes	
Dist	Avail and/or Special
A-1	

APPROVED:



  
Dr. Derek J. Hodgson, Head, Department of Chemistry

Dr. Thomas G. Dunn, Dean of Graduate Studies and Research

Meyer, Howard R., Jr. Studies of Thin Film Chemical Sensors Using the Quartz Crystal Microbalance, Ph.D., Department of Chemistry, August, 1990.

✓ The quartz crystal microbalance (QCM) is emerging as powerful new tool in sensor technology. In the course of this work, the QCM is used to study solvent and ion transport in poly(vinyl chloride) (PVC) ion-selective electrode (ISE) membranes and as a base for thin film analytical sensors for specific ionic species in solution.

Thin (approximately  $1.5\mu\text{m}$ ) PVC-based ISE membranes can be easily attached to the QCM. When these membranes swell in solution due to solvent and/or ion uptake, the resultant mass change in the film causes the resonant frequency of the quartz crystal to decrease. The frequency measurements obtained when exposing ISE-type membranes containing neutral carrier type ionophores to analyte-containing solutions allow one to approximate the mass of solvent and analyte ions that entered the films during sensor operation. QCM mass measurements and conductance analysis of the membranes evaluated in this study indicate that they are extensively hydrated, implying that, at the least, the surface layers of PVC-based ISE membranes are extensively

hydrated. This study therefore gives further insight into the operation of these membrane-based sensors.

To my wife and best friend, Mary, thank you for being there and always encouraging me. I could not have done this without you. To my children, Rachel, Hannah, and Amy, thank you for your love, patience, and support throughout this project.

To my parents, thank you for always believing in me and encouraging me to pursue worthy goals.

*What you do is determined by what you are.  
What you are is determined by what you think.  
What you think is determined by what you learn.  
What you learn is determined by that to which  
you are exposed.*

*Walt Disney*

## ACKNOWLEDGEMENTS

The author wishes to express a special thank you to his mentor, Dr. Daniel A. Buttry. Your help and guidance throughout the course of this work will always be remembered. I chose to work with you because, in the words of Dr. Royce Murray, you are "one of the best." After having learned from and worked with you over the last three years, I *know* he is right.

To Dr. Ricardo Borjas, thank you for your insight and encouragement during this project. Your suggestions proved invaluable more than once. I expect to hear great things of you in the coming years.

To the U.S. Air Force and my country, thank you for making my dream possible.

I thank my Lord and Savior, Jesus Christ, for granting the desires of my heart. Above all else, may I be found a faithful steward.

We are grateful to the Office of Naval Research for generous support of this work.

## TABLE OF CONTENTS

CHAPTER	PAGE
I. INTRODUCTION.....	1
A. Thermal Sensors.....	3
B. Optical Sensors.....	4
C. Mass Sensors.....	6
D. Electrochemical Sensors.....	10
E. Poly(vinyl) Chloride Ion-Selective Electrode Membranes.....	11
II. QUARTZ CRYSTAL MICROBALANCE THEORY AND OPERATION PRINCIPLES.....	19
A. Historical.....	19
B. Quartz Crystals and Oscillator Circuits.....	22
C. Equivalent Circuit Description of the QCM Resonator.....	35
D. Mass-Frequency Relationships for the QCM.....	40
1. Elastic (Solid) Films.....	40
2. Viscous (Liquid) Films.....	44
3. Viscoelastic Films.....	48
E. Other Factors Affecting QCM Response.....	51
1. Temperature.....	51
2. Film Uniformity.....	52
3. Stress Effects.....	55
F. Applications.....	55
G. Conclusion.....	55
III. QUARTZ CRYSTAL MICROBALANCE STUDIES OF SOLVENT AND ION UPTAKE AND RELEASE IN POLY(VINYL) CHLORIDE ION-SELECTIVE ELECTRODE FILMS.....	58
A. Introduction.....	58
B. Experimental.....	63
C. Results and Discussion.....	71
1. The Membranes.....	71
2. The Solutions.....	76



3. Membrane Responses.....	77
4. Conductance Studies.....	83
5. Membrane Sensor Evaluation.....	86
a. Charge Balance and Donnan Failure.....	86
b. Co-ion and Counter-ion Studies.....	90
c. D <sub>2</sub> O Studies.....	92
D. Conclusions.....	93
REFERENCES.....	100

## LIST OF TABLES

	PAGE
Table 2.1    Some applications of the quartz crystal microbalance. Listed beside the application is a primary developer of the application and the year of the development. Additional applications are contained in a fine review by Guilbault.....	56
Table 3.1    Film composition vs. maximum response for 1mM KCl.....	74
Table 3.2    Theoretical versus actual responses for various membrane formulations.....	78
Table 3.3    Summary of frequency responses (in Hz) vs membrane lifetime.....	82
Table 3.4    Conductance ( $F_0$ and $\Delta F$ ) values for membranes.....	85
Table 3.5    Co-ion responses (in Hz) for CE sensor membranes.....	91
Table 3.6    6.4% bisCE sensor membrane responses to D <sub>2</sub> O and 0.1mM Na <sup>+</sup> .....	94

## LIST OF FIGURES

	PAGE
Figure 1.1	a) A thermistor. The material contained inside the glass shell is a mixture of BaO and SrO. b) A pellistor.....5
Figure 1.2	Physical configurations of some optical sensors.....7
Figure 1.3	A surface acoustic wave device. The surface wave is generated at the transmitter, transverses the delay line where it detects mass absorption/desorption in the sensing layer, and is detected at the receiver.....9
Figure 1.4	Two types of electrochemical sensors. a) A potassium ion ISFET. Valinomycin is used as the neutral carrier in this device. b) Conventional and coated wire PVC ion-selective electrodes.....12
Figure 2.1	The piezoelectric effect. a) An unstressed piezoelectric medium. b) Upon compression, the dipoles within the medium move, giving rise to a net electric polarization.....20
Figure 2.2	Common quartz crystal cuts. a) AT-cut. b) BT-cut. c) SC-cut.....24
Figure 2.3	Fundamental oscillation modes for quartz crystals. a) Extensional mode. b) Flexural mode. c) Face shear mode. d) Thickness shear mode (predominant mode in AT-cut crystals).....25

Figure 2.4	Temperature dependence of fundamental oscillation frequency for 5 MHz AT-cut crystals near room temperature.....	26
Figure 2.5	5 MHz AT-cut crystal similar to the ones used in this study.....	29
Figure 2.6	Relative mass sensitivities of AT-cut plane (a) and plano-convex (b) crystals as a function of radial distance from the crystal center.....	31
Figure 2.7	Diagram showing some types of mounting assemblies for circular disk quartz crystals.....	32
Figure 2.8	Schematic for the oscillator circuit used in this study. IC1 = MC1733. R1 = 2.2M $\Omega$ . R2 = 200 $\Omega$ . R3, R4, R5, R6 = 180 $\Omega$ . R7 = 220 $\Omega$ . C1 = 0.01 $\mu$ F. T1, T2 = 2N3904. D1, D2 = HP5082-2811 Schottky diodes.....	33
Figure 2.9	Equivalent circuit diagram for a piezoelectric resonator. See text for discussion of circuit elements.....	36
Figure 2.10	Conductance spectra for a 5 MHz crystal in air and with one side contacting water.....	39
Figure 2.11	Frequency versus film thickness plotted for various $Q_1$ values.....	50
Figure 3.1	Frequency versus time trace for an experimental cycle. Top trace: reference film response. Bottom trace: sensor film response.....	62
Figure 3.2	Top: 5 MHz AT-cut crystal similar to those used in this study. Bottom: Diagram of a PVC film attached to the electrode surface on the crystal.....	65

Figure 3.3	The ionophores used in this study. Top: Dibenzo-18-crown-6, a potassium ionophore. Bottom: Bis[(12-crown-4)-2-ylmethyl]-2-dodecyl-2-methyl malonate, a sodium ionophore.....	66
Figure 3.4	Flow cell used in the experiments. The reference crystal goes in one compartment and the sensor crystal goes in the other. Electrical contact is made with clips attached to the crystals through the oblong access ports on the sides of the cell.....	68
Figure 3.5	Experimental set-up. R, S = Reference and sensor oscillator circuits. These circuits are powered by an HP6205C power supply. The solutions are pumped through the cell at a rate of 3.7 mL/min by a Wiz RP pump. Frequency measurements are made on Philips 6654 frequency counters and recorded on a Kipp and Zonen BD91 (XYY') recorder.....	70
Figure 3.6	A typical (KCl) concentration profile for a 2.2 $\mu$ L thick 1.2% CE film set. Top trace: reference film response. Bottom trace: sensor film response.....	80
Figure 3.7	Conductance spectra for sensor membranes. a. Dry membrane. b. Sensor membrane in water (CE saturated). Note the frequency decrease and spectral broadening in the solvent saturated membrane.....	87
Figure 3.8	KCl Concentration profile for a CE sensor film showing site saturation and incipient Donnan failure. Note that this effect occurs only in the sensor membrane because there is no driving force present (i.e. ionophores) in the reference membrane to pull analyte ions in.....	89

Figure 3.9     Figure illustrating the "three-region  
membrane" model. Relative plasticizer  
concentrations and region resistivities (as  
proposed by Buck<sup>23-25</sup>) are shown.....97

Figure 3.10    Illustration showing reference and sensor  
membranes' responses to analyte solutions.  
a. Reference membrane. Some analyte (and  
accompanying solvent) enters the membrane  
due to the ion exchange capabilities of  
PVC. b. Sensor membrane. A considerable  
amount of analyte (and accompanying  
solvent) enters the membrane due to the  
ionophore *and* PVC ion exchange  
capabilities.....98

## CHAPTER I

### Introduction

The field of analytical chemistry involves several important tasks, among these are detection and quantification of an analyte. Although there are many tools available to the analytical chemist to aid him or her in accomplishing these tasks, some of the simplest to use are chemical sensors. For this reason, chemical sensors are being used in increasingly greater numbers, in applications ranging from routine analyses to "one-shot" warning-type sensors. The use of chemical sensors has in many ways revolutionized the field of analytical chemistry.

Chemical sensing is part of an information acquisition process whereby information about the chemical nature of a sample is provided in real time to the user. It involves the conversion of information about the sample (identity and concentration information) into electronic signals which are processed by associated equipment to give the user the information he desires. This process necessarily involves selectivity since many possible interferences, both physical and chemical, routinely occur in the analysis process. Selectivity for the analyte over as many as

possible of these interferences is absolutely necessary unless the predominant interferences are known to be absent or pretreatment of the sample to remove these interferences is accomplished. Selectivity, referred to in this discussion because specificity (although desirable) is achievable in few instances, is accomplished by use of the sensing species most selective for the analyte.

The physical design of a chemical sensor is extremely important since the sensing species is usually of molecular dimensions or smaller. This requires that the sensing species must be physically coupled to the sensor ensemble in such a way that it remains a part of the sensor ensemble long enough to complete at least one analysis, and preferably to complete hundreds or thousands of analyses. An example of a well known chemical sensor illustrating this concept is the potassium ion-selective electrode. In this sensor, valinomycin (one of the most, if not the most selective ionophores for potassium: the sensing species) is immobilized in a poly(vinyl chloride) (PVC) matrix which is physically attached to an electrode body to form the sensor.

There are three major classes of chemical sensors; optical sensors, mass sensors, and electrochemical sensors. A fourth class, thermal sensors, while operating on the same principles as chemical sensors, relays physical information (its temperature) about a sample only. Each of



these classes will be briefly discussed below, with a pertinent example cited. Since mass and electrochemical sensors have direct impact on the present work, the discussion of these classes will serve only to introduce them, as they will be discussed in greater detail later in the manuscript.

#### A. Thermal Sensors<sup>1</sup>

Thermal sensors sense only the heat content of a sample. There are three major types of these devices; thermistors, pyroelectric devices, and catalytic gas sensors. Thermistors are capable of measuring temperatures in the  $-80^{\circ}\text{C}$  to  $+350^{\circ}\text{C}$  range. Formed by encasing the oxides of semiconductors in a glass shell with two wires providing electrical contact, these devices are actually resistors that change their resistances as a function of temperature. These devices are quite common and have been used in numerous applications. Pyroelectric devices are based upon crystalline materials lacking a center of inversion but having a permanent electric polarization due to the ionic orientation in the crystal. As the temperature changes, the crystal will expand or contract causing the electric polarization within the crystal to change. There have been very few applications of these devices thus far. Catalytic gas sensors, often referred to as pellistors, are one of the simplest types of sensors

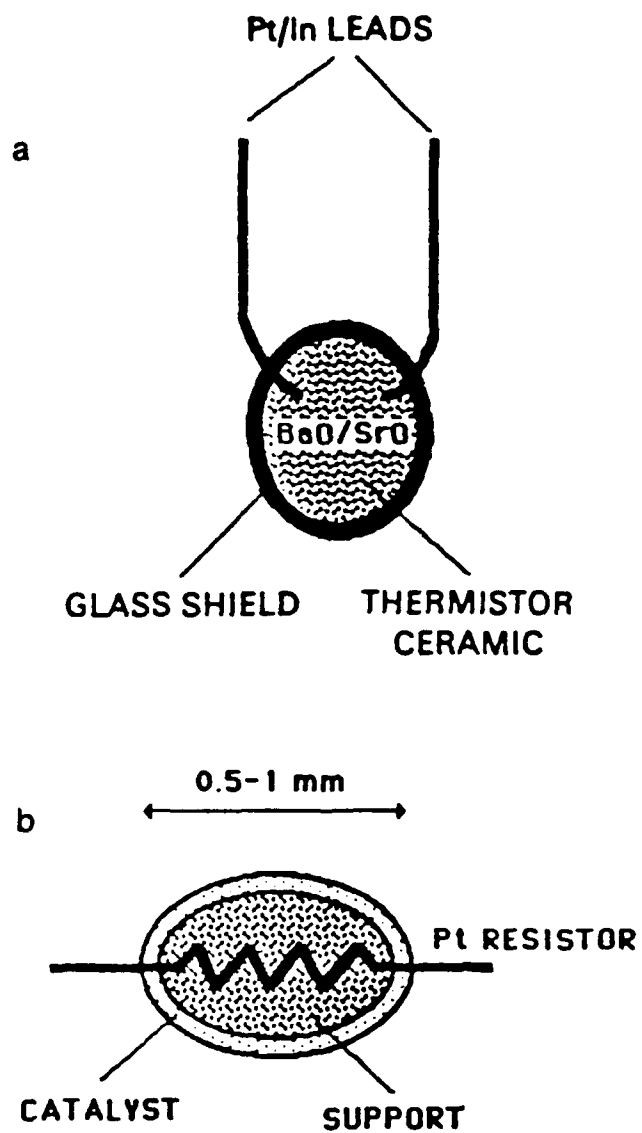


Figure 1.1 a) A thermistor. The material contained inside the glass shell is a mixture of BaO and SrO. b) A pellistor.<sup>1</sup>

available in terms of design and operation. They are constructed of a platinum coil imbedded in a  $\text{ThO}_2/\text{Al}_2\text{O}_3$  pellet which is coated with a porous catalytic metal. When a gas reacts at the catalytic surface, the heat evolved heats the platinum coil, increasing its resistance. These devices are usually connected in a Wheatstone bridge, which provides the output signal. Diagram of a thermistor and a pellistor are shown in Figure 1.1

#### B. Optical Sensors

Operating on the same principles and with much (if not all) of the same equipment as spectrophotometric methods, optical sensors detect the absorption of source radiation or fluorescence caused by the interaction of a sample with a sensing molecule entrapped in a sensing layer on the surface of an optical transmission waveguide. The major differences between optical sensors and spectrophotometers are in their design and their use. In optical sensors, the source radiation is channeled through an optical fiber or waveguide to the sensing area and then to the detector, while mirrors or other optical elements are used to accomplish this in spectrophotometers. Spectrophotometers are designed for input of the sample by the operator, while optical sensors are designed for remote sensing of samples that are physically inaccessible or where removal from their environment would alter their properties (i.e. in

vivo monitoring of cellular fluids during metabolism). Optical sensors are also used in environments where the operation of electrical devices would be hazardous. Optical sensor applications include sensing ionic, biomolecular and gaseous species. Two of the most well known are the pH optrode and CO<sub>2</sub> sensor. Figure 1.2 shows some of the optical geometries used in optical sensors.

### C. Mass Sensors

Mass sensors are based on microbalances, devices based on piezoelectric materials that can translate mass changes into alternating current (AC) frequency signal changes. In these devices, the analyte is detected by adsorption (physisorption or chemisorption) either directly on the device or into a sensing film on the surface of it. The value of these devices is that, because of their high sensitivity and stability, they can detect mass changes on the nanogram to subnanogram level. Selectivity (or specificity, in the case of biomolecular mass sensors) for a specific analyte can be achieved by attaching a film containing a sensing species to the device or by chemically modifying the electrodes on the surface of the device. There are two types of mass sensors, quartz crystal microbalances (QCMs) and surface acoustic wave (SAW) devices. Both utilize a quartz substrate with electrodes on its surface attached to a radio frequency range AC

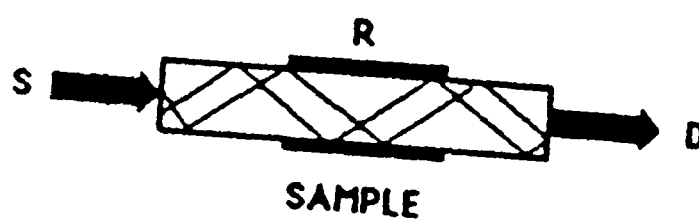
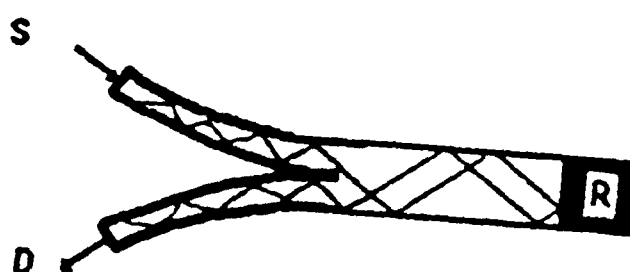
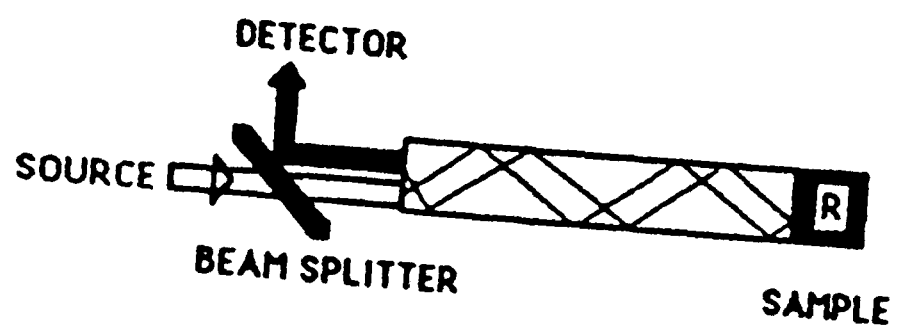


Figure 1.2 Physical configurations of some optical sensors.1

voltage source to drive the devices at their operating frequencies. While greater mass sensitivity is attainable with SAW devices, the relationships between the observed frequencies and mass detected are empirical and SAW devices they are more difficult to operate than QCMs. For this reason, SAW devices have seen little use in sensor applications thus far. Since the QCM is used as an ionic sensor in this study, aspects of QCM-based ionic sensor optimization are discussed below. A SAW device is illustrated in Figure 1.3.

The QCM has successfully been used in sensors of both gaseous and aqueous species, in addition to its original application as a mass deposition sensor in vacuum (solid film) deposition techniques. Guilbault has pioneered work in the area of gas-phase sensors employing the QCM.<sup>34,35</sup> Buttry and Lasky's glucose sensor employing the enzyme hexokinase<sup>36</sup> is one of a few successful applications of the QCM in a solution-based sensor mode.

The major problem one faces in constructing a successful QCM-based ionic sensor is finding an ionophore selective enough for the analyte that interferences will be negligible but will also release the analyte ion quantitatively and rapidly. A "one-shot" sensor would be valuable in a warning device, but aside from such applications, sensor reversibility (quantitative rapid ion release) is essential. The above mentioned glucose sensor

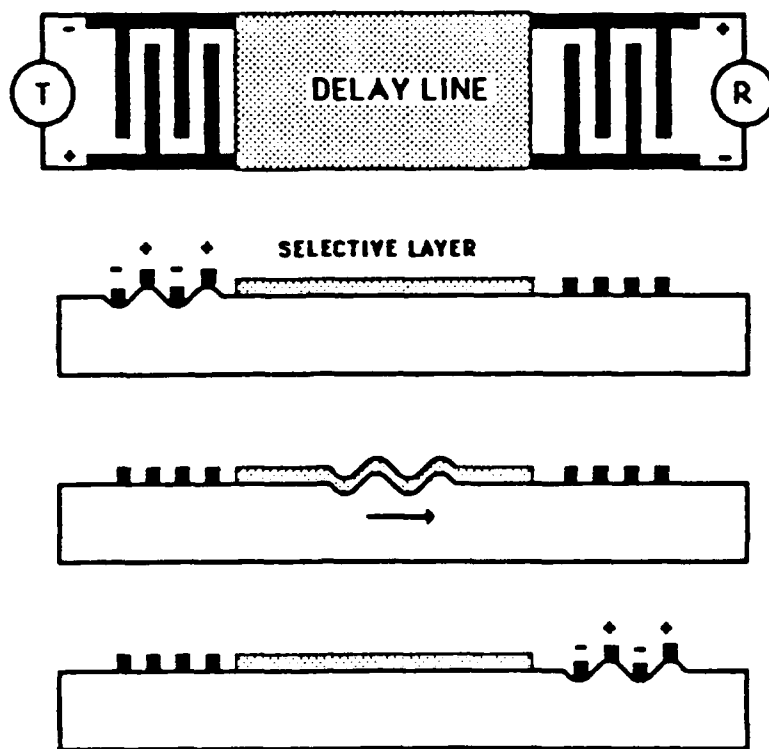


Figure 1.3 A surface acoustic wave device. The surface wave is generated at the transmitter, transverses the delay line where it detects mass absorption/desorption in the sensing layer, and is detected at the receiver.<sup>1</sup>

is successful because it meets these rigid criteria.

Another factor involved in the synthesis of a QCM-based ionic sensor is the method of attachment of the ionophore to the crystal. Although direct binding of the ionophore to the surface would be desirable (to give films thin enough for the Sauerbrey relation to hold rigidly) the dynamic range of such a sensor would be extremely limited, since only a monolayer's worth of the ionophore would be present to detect the analyte. Such a configuration would be possible for a "one-shot" sensor, however. To make a sensor that could have routine applications, one must immobilize the ionophore in a matrix such as PVC (see above). The method of ionophore immobilization (chemical attachment to a polymer, dissolution in the matrix, etc.) is also important, since ionophores that are slightly soluble in water would result in sensors having short operational lifetimes if not confined in the sensor matrix. A detailed discussion of the QCM operation and theory is presented in the Chapter 2.

#### D. Electrochemical Sensors

Electrochemical sensors constitute the oldest and largest class of chemical sensors. In these sensors, electrochemical reaction with the analyte (oxidation-reduction reactions), electrical measurements on the analyte (e.g. resistivity, conductivity, etc.), or chemical



binding or sequestering of the analyte by a sensing layer is used to generate an electric signal related to the type and/or concentration of analyte present. There are several types of electrochemical sensors, but all fall into three major classes based on the type of measurement made: potentiometric sensors (voltage measurement), amperometric sensors (current measurement), and conductometric sensors (conductivity measurement). The best known electrochemical sensors are chemically selective electrodes and chemically selective field effect transistors (CHEMFETs). An ion-selective CHEMFET (ISFET) is illustrated in Figure 1.4.

PVC-based ion-selective electrodes (ISEs) are one of the major types of chemically selective electrodes. Since this study focuses on the sensing films in these sensors, hereafter referred to as PVC ISE membranes, they will be discussed in detail in at this point. Two types of PVC ISEs are shown in Figure 1.4.

#### E. Poly(Vinyl Chloride) Ion-Selective Electrodes Membranes

Poly(vinyl chloride) has successfully been used as a matrix for ion-selective electrodes (ISEs) for over 20 years. ISEs constructed using this material are characterized as robust, having long operational lifetimes, and having excellent sensitivity and reproducibility. These factors, combined with their ease of manufacture and being relatively inexpensive, have contributed to the

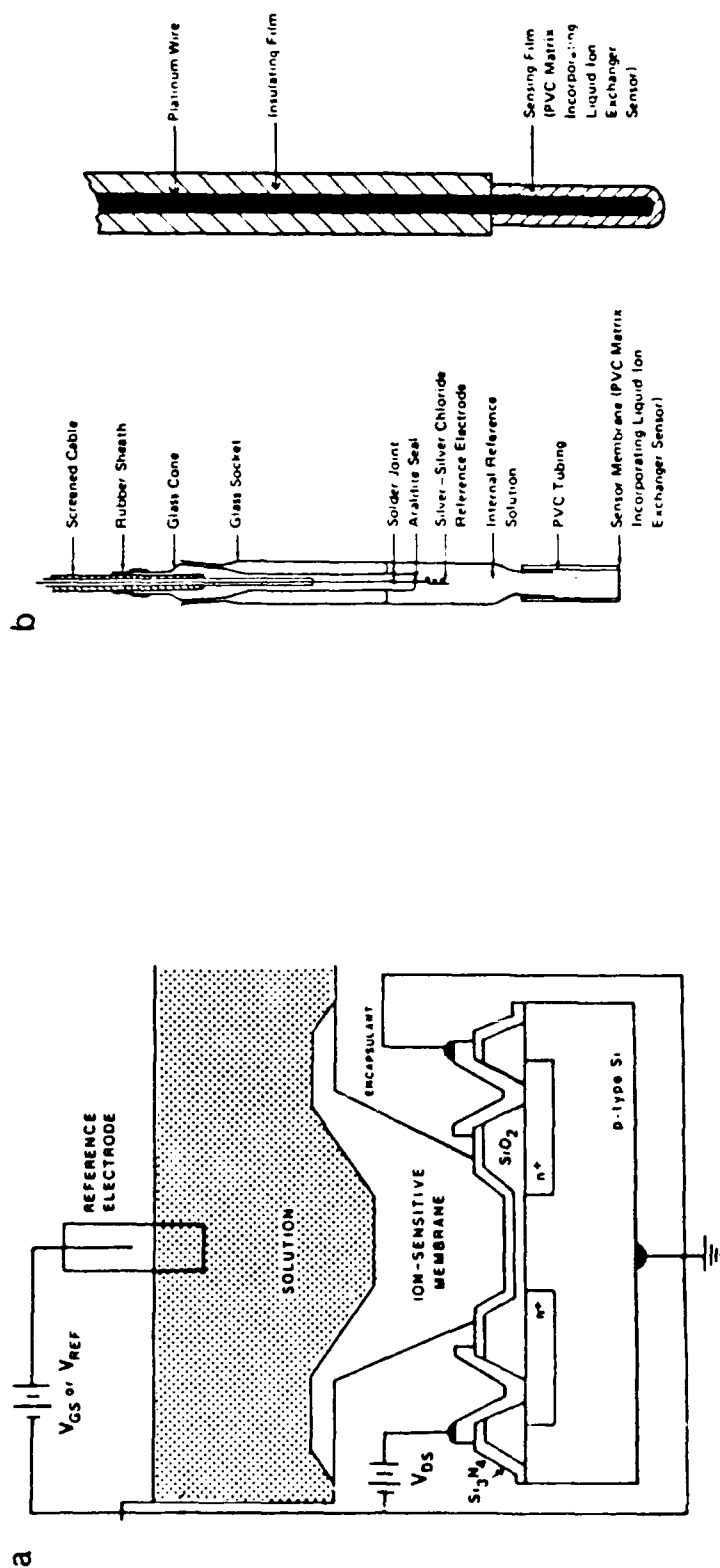


Figure 1.4 Two types of electrochemical sensors. a) A potassium ion ISFET. Valinomycin is used as the neutral carrier in this device.<sup>1</sup> b) Conventional and coated wire PVC ion-selective electrodes.<sup>101</sup>

popularity of the PVC-based ISEs.

Kumins and London<sup>2</sup> conducted the first systematic study of the electrochemistry of PVC membranes in 1960. In their work, they noted that these membranes were cation selective and had low ion-exchange capacities. Shatkay conducted the first studies on PVC as an ISE matrix in 1967.<sup>3</sup> He prepared his membranes by knife coating a mixture of PVC, tri-n-butylphosphate (the plasticizer), and thenoyltrifluoroacetone (the sensing species) over a woven cloth. The interest spurred by Shatkay's work lead to the development of the first "pure PVC" ISE membrane electrodes by Moody, et al,<sup>4-5</sup> in the early 1970's, where they used liquid ion exchangers as the sensing species. Significant progress in the design and theoretical foundation of these ISEs was made during the 1970's, and ISEs for numerous species appeared. The earliest studies involving optimization of the membrane were conducted by Moody, et al, in 1972-4.<sup>6</sup> The membrane formulation they developed is still in use today, and recent studies have confirmed that this formulation is optimal.<sup>7-9,29</sup>

PVC ISEs are almost exclusively of the neutral carrier type. In these ISEs, neutral hydrophobic ionophores are incorporated into the PVC matrix during membrane preparation. Plasticizers, materials added to to increase the workability and flexibility<sup>10</sup> of polymers, are added to dilute the PVC matrix, making the membrane permeable to

ionic species involved in charge transport processes. It is this ionic permeability that permits the establishment of interfacial potential differences at the membrane boundaries, leading to the electrochemical response of the ISE. Plasticizers have a considerable effect upon the performance of PVC ISEs, and the choice of plasticizer one uses can be of major importance.<sup>11,33</sup> PVC does not, however, have a passive role in this process. As has been shown recently, PVC causes ion pairs present in the membrane to be solvent separated<sup>8-9</sup>, thus greatly influencing the performance of these ISEs.

The standard membrane formulation for ISEs, as per Moody's work<sup>6</sup>, is 33% PVC, 66% plasticizer, and 1% neutral carrier. The membranes, typically .1 to 1mm thick, are attached to an electrode body, and the electrode is filled with an internal reference solution of the analyte ion. The reference electrode may also be incorporated into the ISE assembly. Hydrophobic salts (e.g. potassium tetrphenyl borate, KTPB) are routinely added to increase ISE sensitivity by increasing the number of anionic sites within the membrane.<sup>12-14</sup> The role of these sites, as well as the theory of operation of these ISEs is outlined below.

PVC-based neutral carrier ISEs are almost exclusively permselective to cations, as has been confirmed by both potentiometric and transport studies.<sup>15-17</sup> These ISEs show almost complete exclusion of counter-ions, that is ions of

the opposite charge to the analyte. Such counter-ion exclusion is called Donnan exclusion. Since cations can enter the membrane, anionic sites (hereafter referred to as sites) must be present within the membranes to account for charge balance. The presence of these sites in the membrane also hinders anionic permeation of the membrane. The nature and mobilities of the membrane sites (with the exception of the salts mentioned above) is still uncertain.

Numerous studies that have been conducted<sup>15-33</sup> trying to elucidate the ion and charge transport mechanisms of PVC-based ISEs, as well as the nature of the sites within the membranes. Solvent (from analyte solutions) incorporation into the membranes during ionic transport has also been investigated in conjunction with these studies. Results of the major studies are presented below.

The first studies to offer a reasonable hypothesis for the observed cationic specificity (and Donnan exclusion) was conducted by Morf, Simon, et al,<sup>17</sup> in 1976-7. In the first study, they proposed one of the first complete theoretical treatments for PVC ISEs, basing much of their work on the earlier work of Buck and Boles<sup>18</sup>, Lev, et al<sup>19</sup>, and Kedem, Perry, and Bloch<sup>20</sup>. In the second study, they examined ionic transport in PVC-based ISE-type membranes using radiolabelled potassium chloride solutions, with valinomycin as the neutral carrier. In this study, they used a 200 $\mu$ m thick ensemble membrane (consisting of five

40 $\mu$ m thick segments) in a concentration cell. They found  $t_+$ , the transference number for cations, to be  $\sim 1$  and  $t_-$ , the transference number for anions, to be approximately 0, with negligible concentrations of  $\text{Cl}^-$  beyond the first 40 $\mu$ m thick segment. Since almost complete Donnan exclusion of chloride was observed, they postulated that protons from water clusters in the (extensively) hydrated membrane exchanged with  $\text{K}^+$  in solution as the  $\text{K}^+$  was complexed by the valinomycin in the membrane. This resulted in the formation of  $\text{OH}^-$  ions in the water clusters (mobile sites), which were thus responsible for maintaining the electroneutrality of the membrane. This hypothesis was accepted for several years.

In 1982, Sternson, *et al*<sup>21</sup>, postulated that electron rich sites in the plasticizer (e.g. ester, ether, etc. groups) could be responsible for charge balance within these membranes, based on studies using hydrophobic cations. These "sites" were thus quite mobile, and could easily be seen as transport sites for the cations in the membrane. Their treatment did not explain charge transport in the case of hydrophilic cations, however.

Recently, Buck, *et al*, in a series of papers,<sup>23-28</sup> concluded that significant uptake of water did occur in these membranes, but the species responsible for maintaining the electroneutrality of the membranes were indigenous to PVC, being present in it from its time of

manufacture.<sup>23</sup> They used impedance analysis techniques to ascertain the resistances of PVC-based ISE-type membranes with and without added neutral carrier, under various bathing conditions. Two regions of dissimilar resistance were observed, corresponding to a bulk membrane resistance and a very high surface resistance, thought to be due to the formation of a surface layer of exuded plasticizer. In this paper, Buck also proposed that fixed (immobile) sites within the PVC membranes are responsible for the observed charge balance, and that these sites are due to PVC impurities. It is generally thought that the sites are (acidic) organic impurities left over from the PVC manufacturing process, and there is evidence to support this.<sup>29-31</sup>

Armstrong recently stated that there is no evidence for significant uptake of water by these membranes, either as water molecules or as water globules containing OH<sup>-</sup>.<sup>32</sup> He based these remarks on a series of studies where the membrane resistance did not change with time while soaking in water. If extensive water incorporation occurs, the membrane resistance should change as the dielectric constant changes, unless hydration is an extremely fast process (unlikely).

It is with all these thoughts in mind that this project, using the QCM to observe solvent and ion uptake and release from these membranes, was initiated. Although

electrochemical detection by these films is extremely important, this study will not focus on this aspect of PVC-based ISE operation.



## CHAPTER II

### The Quartz Crystal Microbalance

#### A. Historical

The quartz crystal microbalance (QCM) is a relatively new tool to analytical and physical chemistry even though it has been used for over twenty years in vacuum science and technology applications. Based on the converse piezoelectric effect in quartz, the QCM acts as a mass transducer, translating mass losses or gains on the quartz into alternating current frequency (electric) signals that can be detected with sufficiently sensitive electronic equipment.

The piezoelectric effect was discovered in 1880 by Pierre and Jacques Curie.<sup>72</sup> In the piezoelectric effect, a mechanical deformation or strain in a piezoelectric material produces an electric polarization in the material. The effect is only observed in crystalline materials lacking an inversion center of symmetry, and is illustrated in Figure 2.1. In this figure, the mechanical stress (compression) placed on the piezoelectric material causes the electric dipoles in the material to move. The crystalline symmetry is lost and a net electric

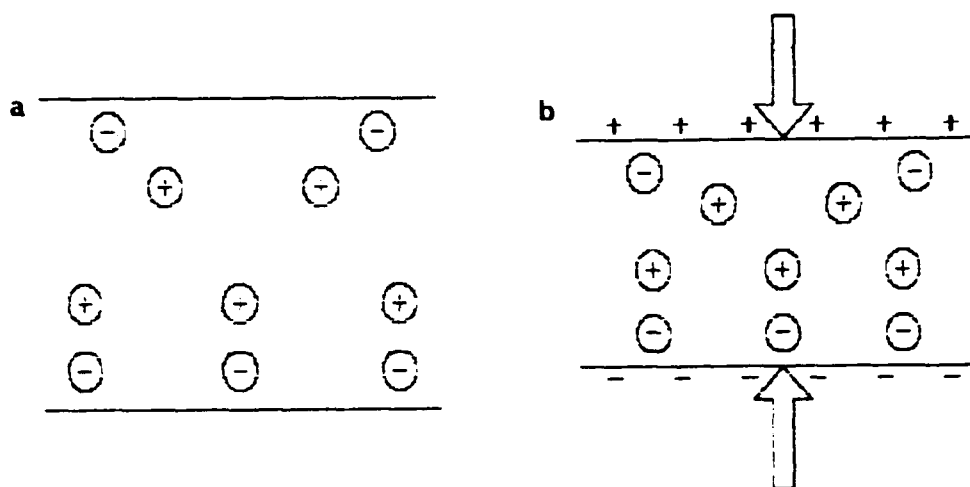


Figure 2.1 The piezoelectric effect. a) An unstressed piezoelectric medium. b) Upon compression, the dipoles within the medium move, giving rise to a net electric polarization.

polarization of the material results. The magnitude of the resultant electric polarization is proportional to stress placed on the crystal. Although crystalline materials in twenty of the thirty-two crystallographic groups are capable of exhibiting the piezoelectric effect, the magnitude of the effect in the vast majority of these materials is too low to be of practical use. Quartz alone provides the necessary mechanical, electrical, chemical and thermal properties to be of technological value in QCM applications.

Within a year of the Curies' discovery, Lippmann predicted the converse piezoelectric effect<sup>72</sup> and the Curies confirmed this later the same year.<sup>72</sup> In this effect, an applied electric field induces mechanical deformation in the piezoelectric material. Alternating current (AC) fields can thus be used to induce periodic oscillation of a suitable substrate. One of the first applications of this effect was in radio, where quartz resonators were used as frequency control devices. These early devices were difficult to operate, however, due to thermally induced frequency "wandering", a function of the crystallographic cut of the quartz material used. The discovery that different crystallographic cuts had different temperature-frequency stabilities was not made until several years after the advent of this technology. With this discovery, the use of quartz crystal frequency

control devices for routine radio applications became feasible.

In the latter 1950's and early 1960's, several advances key to the development of the QCM occurred. Sauerbrey<sup>38</sup> suggested using a quartz resonator as a sensing device for film thickness monitoring in vacuum deposition processes utilizing the converse piezoelectric effect. In his work, he showed that the frequency decrease due to mass deposition on a quartz disk was proportional to the mass deposited for up to 2% mass loadings (the mass deposited caused a frequency change less than 2% of the resonator's original frequency). Frequency measurement to within 1 part in  $10^{10}$  and frequency control to better than 1 part per billion over a several week period became possible during this time. Based on these advances and Sauerbrey's work, the theoretical basis and practical use of the QCM grew significantly. Throughout this discussion, the term resonator is applied to the discrete circuit element, e.g. the quartz crystal, while the term oscillator is applied to the electronic circuit of which the quartz crystal is a component.

#### B. Quartz Crystals and Oscillator Circuits

Due to the advances that have occurred in crystal growth technology, almost all of the piezoelectric quartz devices used today are obtained from synthetically produced

crystals. As mentioned above, the thermal stability of different quartz crystalline "cuts" varies significantly. The fundamental oscillation mode of the quartz resonator (extensional, flexural, etc.) is also influenced by the crystalline cut. These two factors are extremely important because, for QCM mass measurements, an ideal resonator would have only one oscillation mode and would be unaffected by temperature variations. That no crystalline cuts exhibit these characteristics is not unexpected. Cuts having one predominant oscillation mode with undesirable modes suppressed and good frequency/temperature stability are available, and it is these cuts that make piezoelectric devices (including the QCM) practical. The AT- crystalline cut is most widely used, but BT- and SC-cuts (stress compensated; have greater thermal and shock insensitivity) are also being used. Some of the common crystal cuts are illustrated in Figure 2.2.

The quartz resonators (crystals, hereafter) used in this study and in most microbalance applications are of the AT- crystallographic cut. The fundamental oscillation mode for these crystals is the thickness-shear mode, illustrated in Figure 2.3. The temperature dependence of the oscillation frequency near room temperature is generally less than 1 part per million ( $\pm 5$  Hz for a 5 MHz crystal) for these crystals. Their frequency stability over the room temperature range is evident in Figure 2.4 which shows

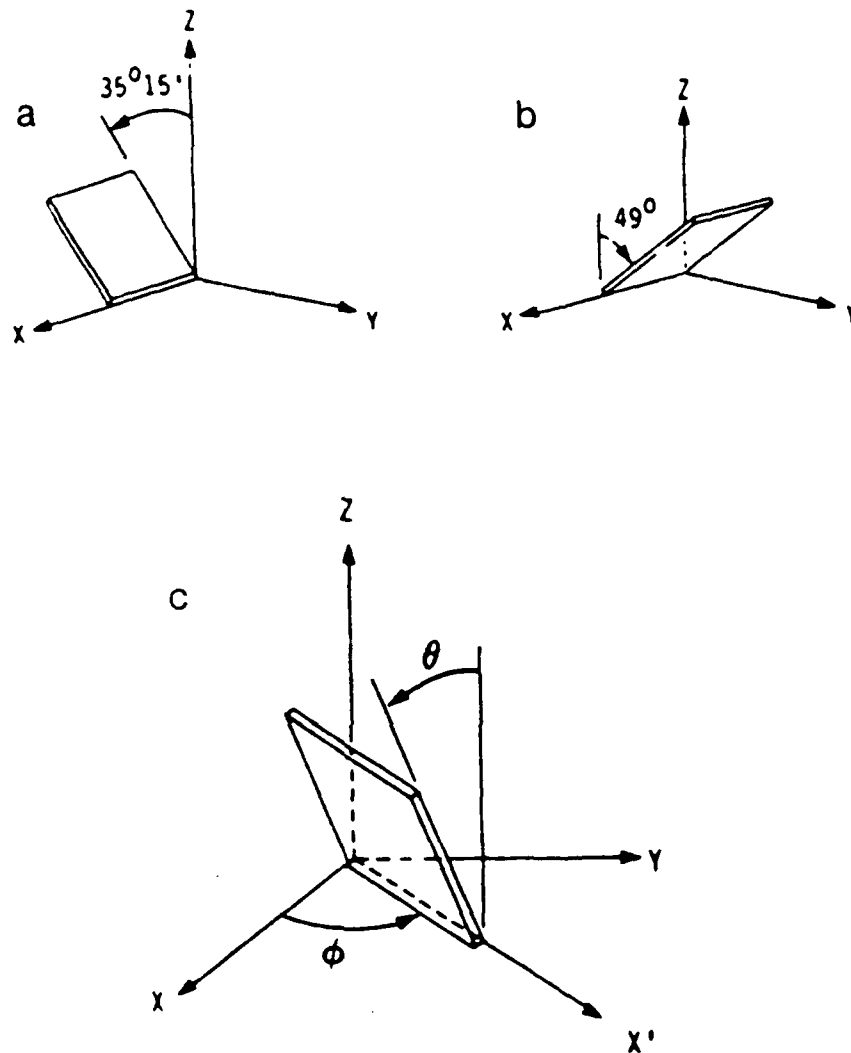


Figure 2.2 Common quartz crystal cuts. a) AT-cut. b) BT-cut. c) SC-cut.<sup>41</sup>

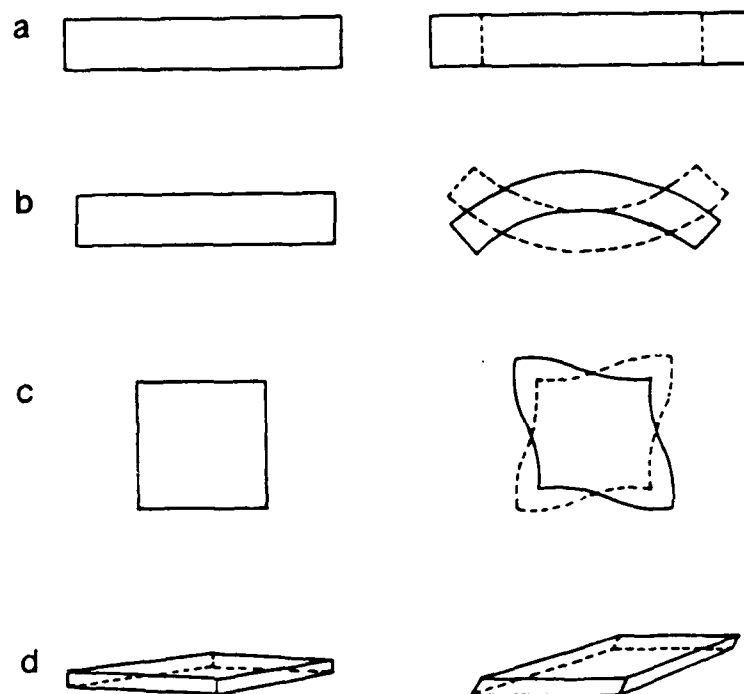


Figure 2.3 Fundamental oscillation modes for quartz crystals. a) Extensional mode. b) Flexural mode. c) Face shear mode. d) Thickness shear mode (predominant mode in AT-cut crystals).<sup>42</sup>

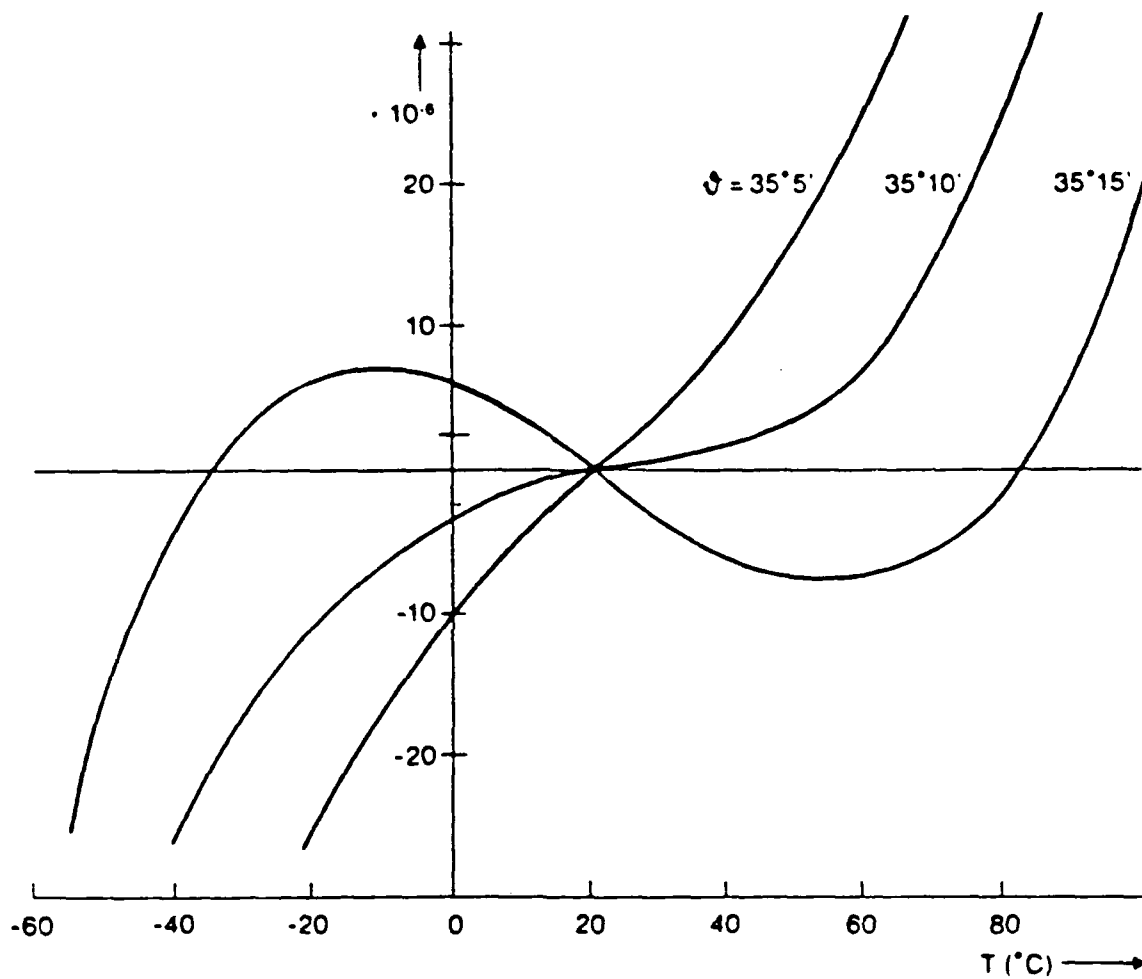


Figure 2.4 Temperature dependence of fundamental oscillation frequency for 5 MHz AT-cut crystals near room temperature.<sup>1</sup>



the temperature dependence for AT-cut crystals as a function of the cut angle. In contrast to the relative stability of AT-cut crystals, X-cut crystals have a temperature coefficient of frequency of  $-20 \text{ Hz/MHz } ^\circ\text{C}$  in this range, meaning the frequency will drop 20 Hz for each  $1^\circ\text{C}$  rise.<sup>3</sup> Slight variations in the cut angle can produce crystals stable in the different temperature regions. Modifications to the oscillator circuit can negate temperature-induced frequency drift as well. Temperature control in the  $\pm 1 \text{ Hz}$  range is practical, and compensation to within less than  $\pm 0.05 \text{ Hz}$  can be achieved with proper oscillator circuit design.<sup>40</sup>

Most QCM crystals are circular disks, although other geometries have been used. For circular AT-cut crystals, plane (both surfaces parallel to within approximately one micron) and plano-convex (with one surface having a very slight radius of curvature) crystals are most commonly used for mass measurements. The plano-convex crystals have a radial mass sensitivity that decreases exponentially as the square of the distance from the center while plane crystals show a simple exponential decrease with distance from the center. As with temperature-dependence, the thickness of a crystal is also dependent upon its crystallographic cut and fundamental resonant frequency. BT-cut crystals are typically 50% thicker than AT-cut crystals of the same resonant frequency.

For AT-cut crystals in an air or vacuum environment, the resonant frequency is inversely proportional to the crystal's thickness. While a 5 MHz AT-cut crystal is approximately 330 microns thick, a 15 MHz crystal is approximately 110 microns thick. Although use of crystals with high resonant frequencies is desired because mass sensitivity increases with the square of the frequency, thinner crystals are more brittle and thus much more difficult to handle. For this reason, most research is done using 1-10 MHz crystals. Greater mass sensitivity using lower frequency crystals can be achieved by utilizing higher harmonics (third, fifth, etc.) of the resonant oscillation, but the oscillator circuitry required to drive the crystal's oscillation is much more complex.

A diagram showing a crystal similar to those used in this study is shown in Figure 2.5. Electrodes (usually gold) are vapor deposited on both sides of the crystal onto either a vapor deposited chromium or silicon underlayer, or, as in this study, a mercaptosilanized quartz (crystal) surface. The underlayer provides better adhesion of the gold electrode to the crystal's surface. The geometry and size of the electrodes and the crystal itself are very important in that they can determine the area of maximum mass sensitivity on the QCM crystal as well as contribute to the suppression of unwanted vibrational modes.<sup>38,42,43</sup> The area of maximum mass sensitivity is almost completely

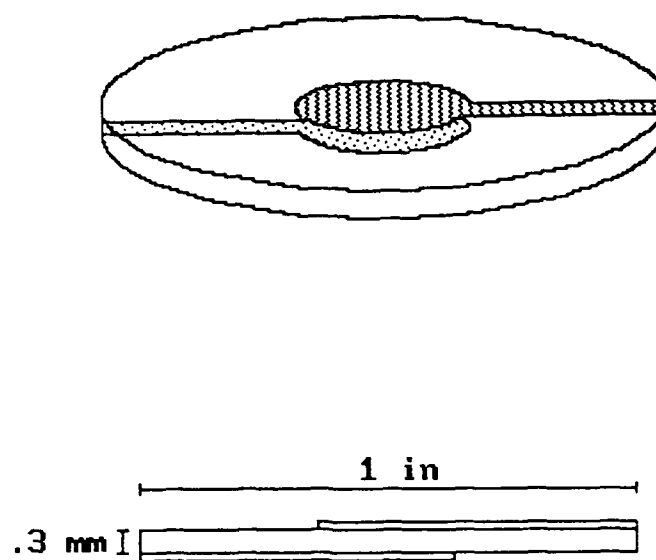


Figure 2.5 5 MHz AT-cut crystal similar to the ones used in this study.

confined to the region between the electrodes, since the shear wave amplitude will be greatest in this region. The mass sensitivity falls off in an exponential manner outside this region, with plano-convex crystals having the greater fall-off rate. Radial mass sensitivities (relative) for plane and plano-convex AT-cut crystals are shown in Figure 2.6.

The method of crystal mounting in the experimental cell can also have a significant effect upon oscillation modes of the quartz crystal due to differing stresses placed on the crystal by the mounts. The major requirement for a mounting assembly is that it must not become a part of the resonator ensemble, as it would then absorb energy thus altering observed frequency changes. For circular quartz (disk) resonators, the most convenient support is around its circumference since the vibration needs to be localized in the center of the crystal. When a suitable support is used, the above mentioned effects are almost negligible. Several different mounting assemblies are shown in Figure 2.7.

The QCM oscillator circuit has two important requirements; sufficient gain and electronic stability to ensure oscillation of the crystal in a viscous medium. A typical oscillator circuit, similar to the one used in this study, is illustrated in Figure 2.8. The operational amplifier used in this circuit, a Motorola MC1733, is wired

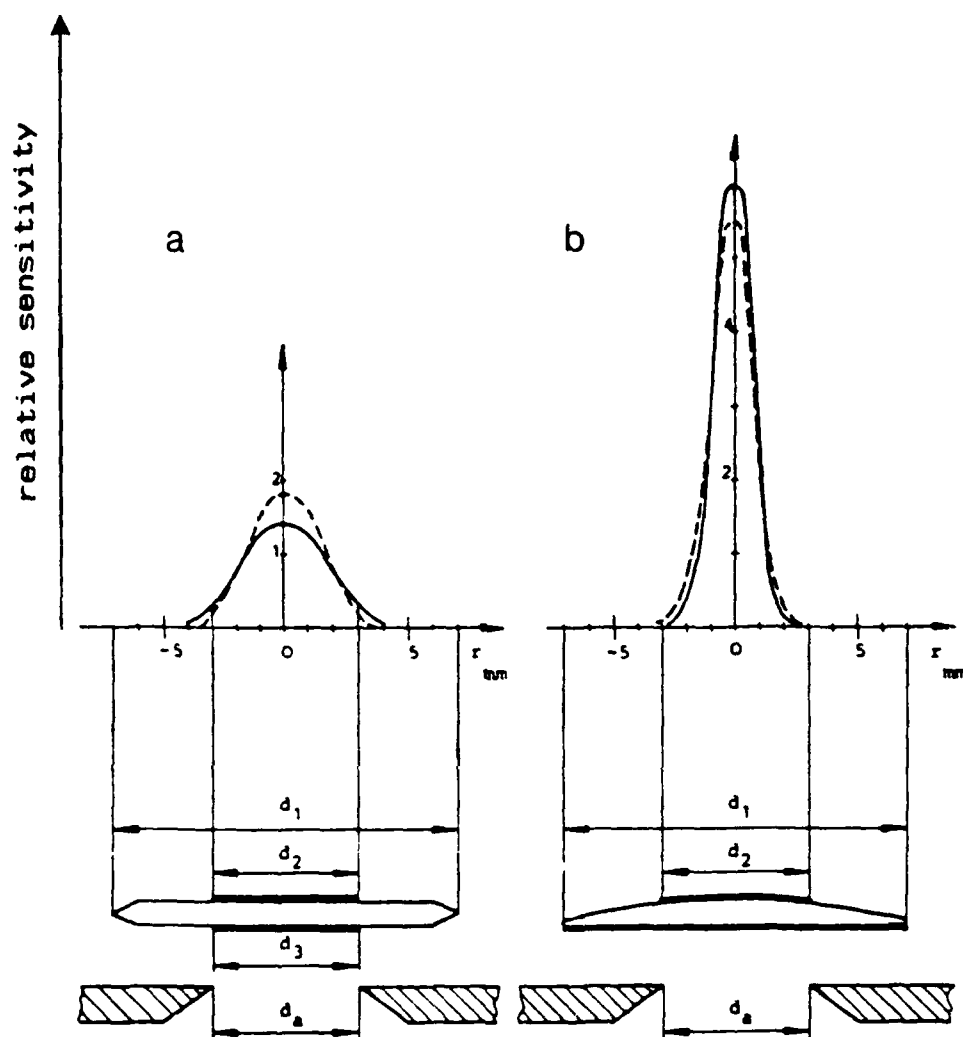


Figure 2.6 Relative mass sensitivities of AT-cut plane (a) and plano-convex (b) crystals as a function of radial distance from the crystal center.<sup>73</sup>



Figure 2.7 Diagram showing some types of mounting assemblies for circular disk quartz crystals.<sup>45</sup>

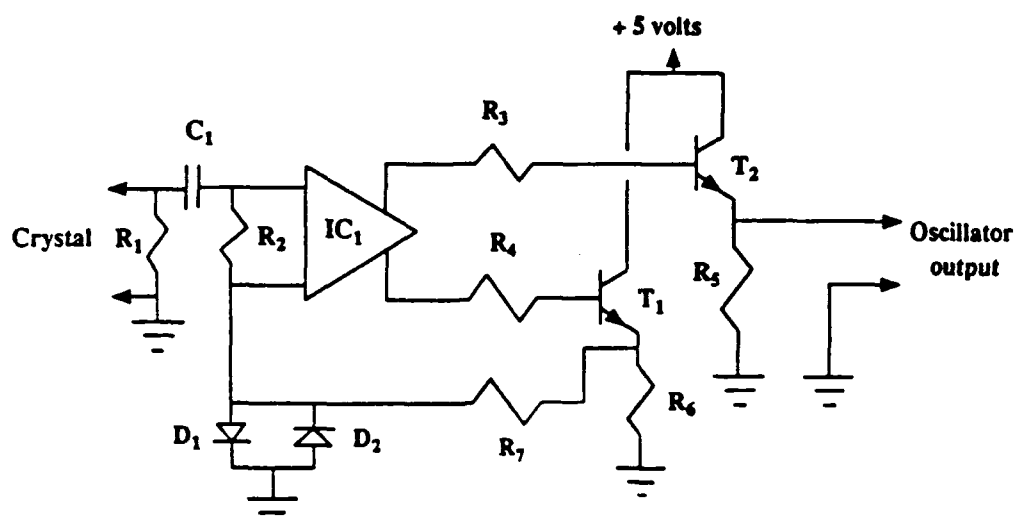


Figure 2.8 Schematic for the oscillator circuit used in this study. IC1 = MC1733. R1 =  $2.2\text{M}\Omega$ . R2 =  $200\Omega$ . R3, R4, R5, R6 =  $180\Omega$ . R7 =  $220\Omega$ . C1 =  $0.01\mu\text{F}$ . T1, T2 = 2N3904. D1, D2 = HP5082-2811 Schottky diodes.

for maximum gain ( $\times 400$ ), and the switching transistor in the feedback loop accomplishes the signal inversion needed to achieve oscillation. This circuit provides a relatively constant 0.4V peak-to-peak across the crystal using a 3.5V DC power supply, even with varying analyte viscosity.<sup>44</sup> The output of the circuit can be sent to a frequency counter (then to a recorder) or a computer for automated experiment control. The equipment used in this study will be fully described later.

Lu lists six criteria governing the usefulness of a vibrational system for mass determinations.<sup>38</sup> (1) The vibrational system should be easily excited, preferably by electric means. (2) A frequency measuring device must be easily coupled to the vibrational system without significantly perturbing it. (3) The resonant frequency of the vibrational system must be sharp and well defined so precise determination of the resonant frequency can be accomplished in a relatively short period of time. (4) The mass induced frequency change must be larger than the signal-to-noise ratio in the oscillator system. (5) The resonant frequency changes due to environmental factors (fluctuations in temperature, pressure, local magnetic and/or electric fields, etc.) must be small in comparison with the mass-induced resonant frequency changes. (6) An equation relating the observed frequency changes to the corresponding mass changes must be known for the



vibrational system. These requirements can be met with high frequency quartz resonators, although exact frequency change-mass change correlation, though desirable, is not a necessity, as will be seen later.

### C. Equivalent Circuit Description of the QCM Resonator

From the discussion above and Figure 2.8, it is obvious that the quartz crystal itself is a discrete element in the oscillator circuit. Several years before the discovery of the piezoelectric resonator, it was shown that a mechanically vibrating system driven by an electric field could be represented by the electric network illustrated in Figure 2.9. The relationships between the parameters of this network and the physical properties of piezoelectric materials were developed soon after the discovery of the resonator in the mid-1920s.<sup>39</sup> For an AT-cut crystal (with unwanted oscillation modes in the immediate vicinity of its resonant frequency suppressed), the equivalent circuit in Figure 2.9 effectively models the resonator's behavior. In this circuit,  $C_0$  is the capacitance of the capacitor formed by the electrodes sandwiching the quartz crystal (does not change during QCM measurements),  $L_1$  is related to the mass displaced during the oscillation,  $C_1$  is related to the elasticities of the crystal and contacting medium, and  $R_1$  corresponds to oscillation energy losses due to the contacting medium,

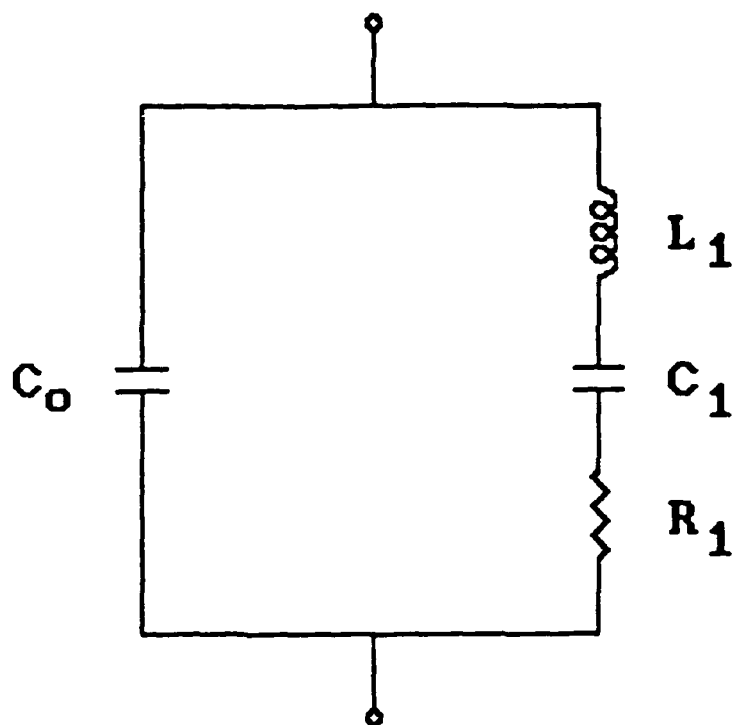


Figure 2.9 Equivalent circuit diagram for a piezoelectric resonator. See text for discussion of circuit elements.

the crystal's mounting structures, and internal friction in the crystal.

Conductance and impedance studies of the crystal resonator (without and with contacting media) reveal important information about the crystal itself and the contacting media. These measurements are made using a network analyzer, bridge methods, or an impedance analyzer as in this study. The frequency at which the conductance (real part of the admittance) is maximum,  $f_s$ , is the resonant frequency of the motional branch of the circuit. This is the frequency normally associated with microbalance measurements. The sharpness of the conductance peak is measured by the  $Q$  value (quality factor) of the crystal. ( $Q$  value measurements are routinely used in electronic analysis of LRC and resonator circuits, with higher  $Q$  values indicating "better" (higher quality) circuit elements.) The sharper the conductance peak, the higher a crystal's  $Q$  value. Sharp conductance peaks (high  $Q$  values) indicate that the attached film is more rigid, while broadened conductance peaks are indicative of viscous losses occurring in an attached film or into a contacting solution.

When the current flowing through the crystal is exactly in phase with the applied voltage, the frequency of zero phase,  $f_r$ , occurs. With an impedance analyzer, as was used in this study, the conductance,  $G$  (real part of the

admittance), reactance,  $X_e$ , resistance,  $R_e$ , and phase angle,  $\theta$ , are measured while the AC voltage frequency is swept.  $R_1$  is approximately equal to  $R_e$  at the frequency where  $X_e$  is zero (slightly above  $f_s$ ), and  $C_0$  is measured at any frequency far removed from  $f_s$ . With these values, the values of  $R_1$ ,  $C_1$ ,  $L_1$ ,  $f_r$ ,  $f_s$  and  $Q$  can be determined using equations 2.1 through 2.5 below.

$$f_s = [2\pi(L_1 C_1)]^{1/2}^{-1} \quad (2.1)$$

$$Q = 2\pi f_s L_1 / C_1 \quad (2.2)$$

$$(f_r - f_s) / f_s = r / (2Q^2) \quad (2.3)$$

$$r = C_0 / C_1 \quad (2.4)$$

$$C_1 = (f_r - f_s)(2\pi^2 f_s^3 C_0 R_1^2)^{-1} \quad (2.5)$$

where  $r$  is the capacitance ratio.<sup>37,39,44</sup>

Conductance spectra for an AT-cut crystal in air and with one side contacting water are shown in Figure 2.10. That energy losses due to the water contacting the crystal significantly shift  $f_s$  and broaden the conductance peak is readily apparent. The full width half maximum (FWHM) value of the conductance peak, referred to as  $\Delta F$ , can be used as qualitative measure of the rigidity of films attached to the crystal. When the viscosity (or viscoelasticity with polymeric films) of the contacting film or medium becomes too great,  $R_1$  will be quite large (greater than ca. 3000 $\Omega$  for 5 MHz for AT-cut crystals) and the crystal will cease to oscillate. For more detailed discussions of the equivalent circuit parameters and

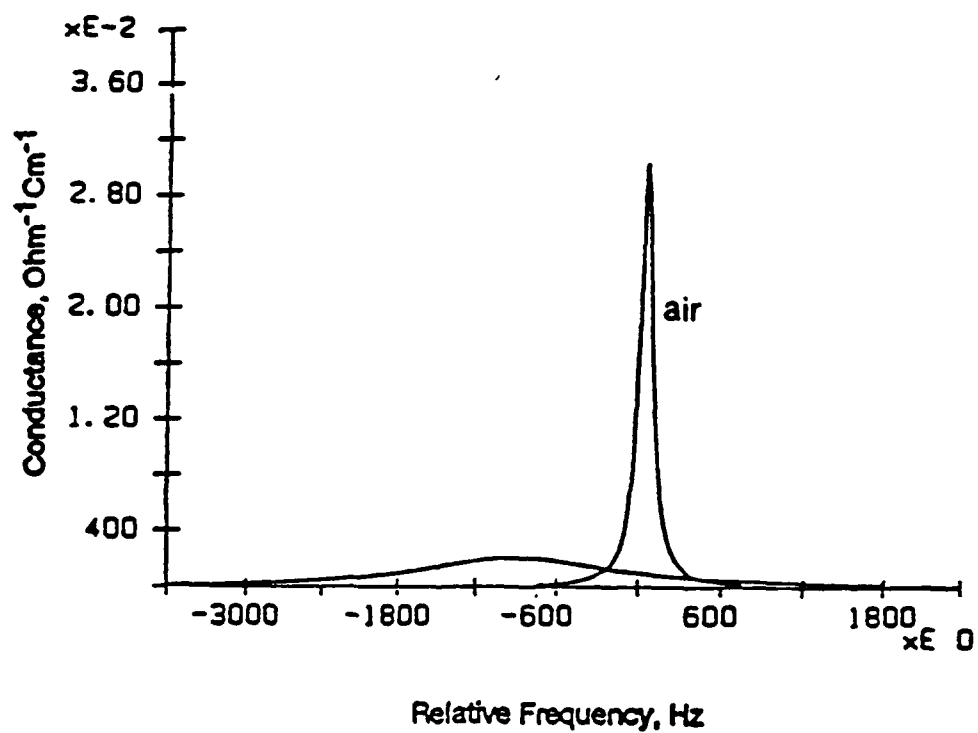


Figure 2.10 Conductance spectra for a 5 MHz crystal in air and with one side contacting water.<sup>46</sup>

analyses, refer to references 1, 3, and 8.

#### D. Mass-Frequency Relationships for the QCM

The theoretical foundation for the QCM can be traced to Lord Raleigh's work showing that a small change in the inertia of a mechanically vibrating system perturbs the resonant frequency of the system.<sup>74</sup> The resonant frequency of a crystal resonator is therefore determined by, along with other physical parameters of the system, the total mass of the resonator ensemble. Ham radio operators have utilized this knowledge for years, changing the resonant frequency of their crystal oscillators by making pencil marks on their surface (mass increases, frequency decreases) or "shaving" the crystal (mass decreases, frequency increases). It is this fact that makes frequency-based mass determination with the quartz crystal microbalance possible.

##### 1. Elastic (Solid) Films

Since mass determinations are made utilizing these resonant frequency changes, the absolute accuracy in the mass determinations is determined by three factors; errors introduced by the frequency or time measurement employed, errors due to resonant frequency changes caused by factors other than mass (e.g. temperature effects), and the accuracy of the formula used to convert the frequency

changes into mass.<sup>40</sup> The first two factors could be effectively minimized by use of available equipment and techniques (crystal cuts, etc.). Sauerbrey developed an analytically useful equation for the QCM in his pioneering work in 1959 by assuming that the mass change of the crystal resonator caused by film deposition on it was equivalent to a mass change in the crystal itself (the film was thin and as dense as quartz).<sup>38</sup> This equation proved to be accurate for up to 2% mass loadings. In the equation,

$$d_f t_f = m_f = -(f_c - f_q) d_q v_q / 2f_q^2 \quad (2.6)$$

$d_f$ ,  $t_f$ , and  $m_f$  are the density, thickness, and mass of the deposited film,  $f_c$  is the resonant frequency of the crystal with the film deposit, and  $f_q$ ,  $d_q$ , and  $v_q$  are the resonant frequency, density, and shear wave velocity in the bare crystal. Since the latter three values vary little near room temperature for AT-cut crystals, they are combined to give

$$C_f = 2f_q^2 / (d_q v_q) \quad (2.7)$$

$$\delta f = -C_f \delta m \quad (2.8)$$

$C_f$  is the calibration constant or mass sensitivity of a QCM and  $\delta m$  is the areal density (mass per unit area) of the film deposit. Equation 2.8 is known as the Sauerbrey equation. The validity of this equation was confirmed by several investigators using crystals with different resonant frequencies and different film deposits shortly after Sauerbrey's initial work. It holds only when the

frequency change for rigid films attached to the resonator surface is small in comparison to the resonant frequency of the crystal (known as the "rigid layer approximation"<sup>47</sup> or "thin film limit").

While this treatment provided an equation that was useful, the assumption that the density of the deposited film was the same as the quartz crystal needed theoretical justification. Neglected effects such as temperature changes, mechanical (clamping) stresses on the crystal perturbing the shear wave, and damping in the oscillator circuit needed to be addressed. Finally, to extend the usefulness of the technique outside the realm of vacuum chamber vapor (metal) deposition work, an equation addressing thicker film deposits and film deposits that were viscous or viscoelastic was needed.

In an attempt to provide a theoretical justification for Sauerbrey's assumption, Stockbridge<sup>48</sup> employed a perturbation analysis technique for a one-dimensional mechanical vibrator, assuming that the acoustic waves did not propagate into the film. By neglecting second and higher order terms in his power series expansion, he obtained Sauerbrey's result, but with increasing film thickness his assumption became less plausible.

Miller and Bolef<sup>49</sup> addressed this problem by treating the entire system (crystal and film) as a composite resonator with only small acoustic losses. That the



deposit is almost perfectly elastic is inherent to this assumption. The major improvement they made was taking into account the properties of the deposited film, which in almost all cases were considerably different from those of quartz. Lu and Lewis<sup>50</sup> extended their work and simplified their result, developing a simple equation relating the frequency change to the mass change due to the film deposition. Their equation is

$$\tan(\pi f_c / f_o) = -(z_f / z_q) \tan(\pi f_c / f_f) \quad (2.9)$$

where  $f_c$ ,  $f_o$ , and  $f_f$  are the resonant frequencies for the composite crystal-film resonator, the crystal, and the film.  $z_f$  and  $z_q$ , the acoustic impedances of the film and the quartz, are

$$z_f = d_f v_f = (d_f \mu_f)^{1/2} \quad (2.10)$$

$$z_q = d_q v_q = (d_q \mu_q)^{1/2} \quad (2.11)$$

where  $v_f$  and  $v_q$  are the velocities of the acoustic waves in the film and quartz, and  $\mu_f$  and  $\mu_q$  are the shear moduli of the film and quartz. The degree to which the frequency changes calculated by Sauerbrey's equation (equation 2.8) deviates from the more accurate equation 2.9 depends on the  $z_f/z_q$  ratio. When the film is quartz, Sauerbrey's equation results. By including the film's acoustic properties in the calculation, they extended the linear mass change-frequency change range from 2% of  $f_o$  to over 40% of  $f_o$  for films other than quartz. It is only accurate with higher mass loadings (frequency changes greater than ca. 10% of

$f_0$ ) however. With lower mass loadings, the  $(z_f/z_q)$  ratio in equation 2.9 will can more closely approach 1 (since  $z_f$  is also a function of the film's thickness) and equation 2.9 will reduce to Sauerbrey's equation (equation 2.8). The analysis of frequency changes by using the acoustic impedances of quartz and film which they introduced is known as the Z-match method.

Benes<sup>51</sup>, utilizing the knowledge that the solutions afforded by Miller and Bolef's (and Lu and Lewis') work included harmonics of the resonant frequencies, used the first and third harmonic frequency responses of the crystals to obtain more realistic acoustic impedance values for the deposit films. He noted a systematic deviation of his calculated  $z_f$  values from the true values, indicating the need for an improved composite resonator analysis. Calculated  $z_f$  values can be used in equation 2.9, however, to give more accurate results.

## 2. Viscous (Liquid) Films

All of the treatments up to this point have dealt with elastic (solid) films. It was long thought that crystals would not oscillate in liquids since the acoustic losses due to solution viscous damping would cause frequency shifts and concurrent loss in the quality value  $Q$  to result in resonator instability and cessation of oscillation. Analytical applications of the QCM were thus limited to

vacuum environments, with the exception of a few gas phase sensors that were developed.<sup>52,53</sup> Glassford<sup>54</sup> was the first to examine acoustic losses in liquids examining shear wave velocity distributions in silicone oil droplets and films on the surface of a QCM. In his treatment, acoustic losses were assumed to occur over a fairly large distance (greater than ca. 50  $\mu\text{m}$ ), with the shear wave velocity distribution decreasing exponentially with increasing distance from the resonator surface. In the thin film limit, where the frequency change for a rigid layer is negligible (less than 2%) compared to the resonant frequency, the mass sensitivity was equal to that attainable in vacuum measurements. Equations for QCM response of liquids relative to solids were derived. In studies of thin (ca. 10  $\mu\text{m}$ ) liquid film sensors and use of the QCM as a LC detector, Nomura<sup>55,56</sup> and Konash and Bastiaans<sup>57</sup> found that crystal oscillation could be maintained when only one face of the crystal was exposed to a liquid and that surface adsorption and desorption effects could be detected. Bruckenstein and Shay<sup>58</sup> made practical use of the QCM in solution in an electrochemical application of the QCM (EQCM), studying electrodeposition of silver under both potentiostatic and galvanostatic conditions. They noted that perturbations in the double layer structure during electrodeposition, which caused the mass of solvent and all dissolved species in the double

layer to change, were responsible for the frequency changes they observed. This implied that the double layer was "firmly attached", e.g. a quasi-rigid film, to the electrode surface, falling within the "no-slip plane" of macroscopic hydrodynamics (referred to as the shear plane in colloid and polymer science, and hereafter). In these treatments, viscous (or viscoelastic) material within a region of finite thickness (usually a few angstroms) immediately adjacent to a surface behaves as if it is a rigid layer, and transition to bulk viscosity (or viscoelastic behavior) occurs outside this region.<sup>59</sup> The QCM therefore weighed all material within the compact layer, and the outer Helmholtz plane (OHP) formed the boundary of the shear plane. Bruckenstein and Shay's result correlated well with the work of Mpandou and Siffert<sup>60</sup> who determined the distance between the OHP and shear plane to be ca. 4 angstroms by zeta-potential measurements.

Kanazawa and Gordon<sup>61,62</sup> conducted the first in-depth theoretical analysis for the case of a QCM with one face in full contact with a solution. In this treatment, they showed that the (crystal) shear wave perturbs only the few microns ( $2.5 \mu\text{m}$  for water) of the contacting solution. Using the fundamental frequency solution for both the Helmholtz wave equation for the crystal at the resonator surface and the corresponding differential equation for the

contacting fluid velocity, they developed an equation,

$$\delta f = -f_0^{3/2}(d_1 n_1 / \pi d \mu)^{1/2} \quad (2.12)$$

where  $d_1$  and  $n_1$  are the density and viscosity of the contacting liquid and  $d_q$  and  $\mu_q$  are the density and shear modulus of quartz, which gave excellent agreement with experimentally determined  $\delta f$  values for glucose and ethanol solutions of varying concentrations. Their treatment now allowed application of the QCM in viscous (liquid) environments with good results. The validity of these results in water and aqueous solutions of various organic compounds was recently confirmed by Kurosawa, *et al.*<sup>75</sup> In this study, however, they noted a deviation of the observed frequencies from values predicted by equation 2.12 for electrolyte and polymer solutions. They hypothesized that double layer effects in the electrolyte solutions and static versus dynamic (high frequency) viscosity differences in the polymer solutions were responsible for the observed deviations. They also noted that the oscillator circuitry employed affects the frequency change observed in solution (i.e. different TTL circuits gave different frequency change values).

In an interesting side light to Kanazawa's developments, Muramatsu, *et al.*,<sup>63</sup> recently used impedance analysis techniques to study solution properties with the QCM. Their results showed excellent linearity of  $R_1$  (of the equivalent circuit) with  $(dn)^{1/2}$ . The value of  $R_1$ ,

easily attainable in conductance analysis experiments, can therefore serve as a good measure of (liquid) film viscous loading effects.

### 3. Viscoelastic Films

While rigid solid films are very elastic and liquids are quite viscous, many compounds, e.g. glasses and polymers, exhibit both elastic and viscous properties simultaneously. For these materials, their viscosity and shear moduli (measure of rigidity or stiffness) are functions of the excitation frequency at which they are measured. In general, the viscosity of these materials tends to decrease with frequency while their shear moduli tend to increase with frequency.<sup>64</sup> In the MHz frequency range, these materials therefore have shear moduli less than that of quartz (because they are less rigid than quartz) and have greater viscosities than quartz (possibly due to viscous loss due to translational motions of the chains relative to one another). For polymeric films, the glass transition temperature  $T_g$  (the temperature range over which the transition from crystalline to glassy structure occurs) will strongly influence film properties and the magnitude of the acoustic losses as well.<sup>44</sup> Acoustic losses in these systems are therefore significantly greater than in viscous media, and solution of the QCM frequency change relationship is significantly more complex.

Kanazawa<sup>65</sup> was the first to address the solution of the problem of acoustic losses in viscoelastic media. In his treatment, he derives an extremely complex equation for the observed frequency in terms of the shear modulus and density of quartz and the density, viscosity, shear modulus, and thickness of the viscoelastic overlayer by using the general solution for the wave equation for shear waves in viscoelastic media. This equation reduces to Lu and Lewis's result in the purely elastic limit and to Kanazawa and Gordon's equation in the limit of purely viscous behavior. He also defines a term,  $Q_1$ , a complex function of the viscosity, shear modulus, density, and film thickness, which is used to study frequency changes in viscoelastic films as a function of film thickness. Plotting film thickness versus the observed frequency change for films with different  $Q_1$  values reveals that strong deviations from linearity (film thickness vs. frequency) can be expected for different film compositions and thicknesses.

A plot of film thickness versus frequency for various  $Q_1$  values is shown in Figure 2.11. In this figure, very small changes in film thickness result in vastly different frequency responses for films of identical composition. This fact has significant implications for the present work.

Recently, Reed, Kanazawa, and Kaufman<sup>66</sup> were able to

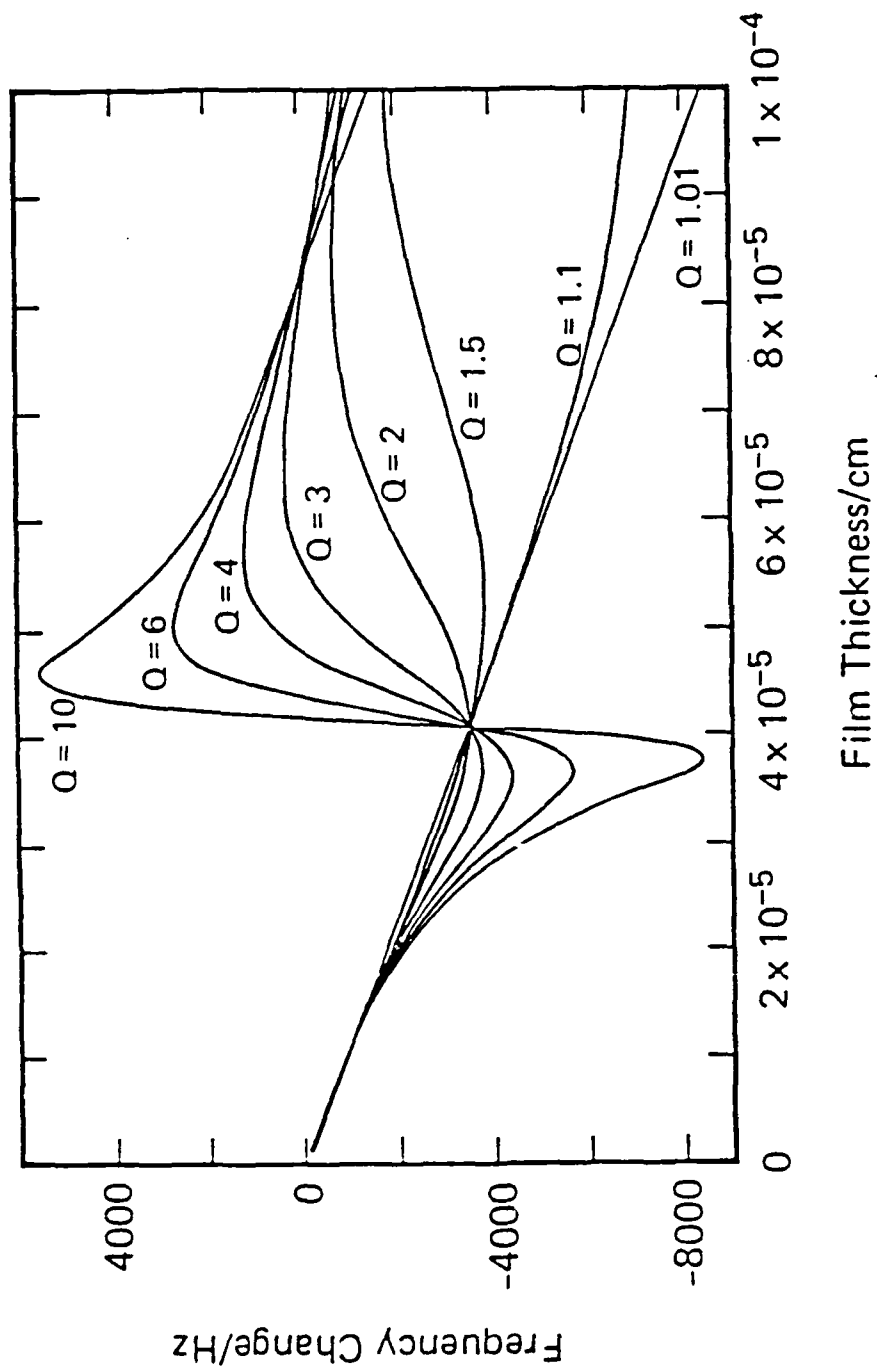


Figure 2.11 Frequency versus film thickness plotted for various  $Q_1$  values.<sup>65</sup>



relate the complete admittance spectrum of a composite resonator (crystal film ensemble) to the film material properties. This study opened the possibility of detailed studies of film properties.

#### E. Other Factors Affecting QCM Frequency Response

In addition to the type of film attached to the crystal surface, there are several factors which can affect the frequency response of the QCM. Some of the more important factors are briefly discussed below.

##### 1. Temperature

Frequency changes induced by the temperature-frequency drift characteristics inherent in different quartz crystalline cuts have been covered earlier. These temperature changes effects can be minimized, if not virtually eliminated, through strategies mentioned above. Temperature effects are not limited to the quartz crystal, however. Temperature changes affect the properties of the film and/or solution contacting the crystal as well and as these properties (viscosity, density, thickness, and shear modulus) of the contacting medium change, its acoustic impedance changes. For a crystal with one side in contact with water, Donohue and Buttry observed frequency changes as large as 30 Hz per degree over the 10°-50°C temperature range.<sup>67</sup> While a changes of this magnitude may not appear

significant in relation to the crystal resonant frequency, it is larger (in some cases several times larger) than the frequency changes expected for processes such as monolayer adsorption and desorption processes, and definitely not negligible in studies of solvent and ionic transport in thin films adsorbed to the quartz crystal. Similar effects can be seen in viscoelastic films attached to the QCM crystal, and in cases where such films are immersed in solution. For this reason, thermostatic temperature control to within at least  $\pm 1.0^\circ\text{C}$  (preferably to better than  $\pm 0.02^\circ\text{C}$ ) is required for experiments where the frequency is to be monitored for long periods of time.<sup>44</sup> For shorter duration experiments, such control is not necessary since the temperature changes will be very small during the experimental cycle.

## 2. Film Uniformity

For the equations relating observed frequency changes to mass changes at the crystal surface to be valid, the thickness and density of the film deposit must be uniform. This is required because the mass changes (indirectly) observed in QCM measurements are actually *areal density* changes, that is, changes in the mass per unit area on the crystal surface. If a film on a crystal is not both homogeneous and uniformly thick, areal mass changes will differ from site to site over the film causing the

frequency sensitivity to vary similarly.

If the film is of uniform thickness but its surface is roughened ("scratched" or rippled), solvent can become trapped in pockets in the film. Schumacher, et al.,<sup>68,69</sup> observed this effect for gold, silver and copper electrodes electrochemically oxidized in neutral and alkaline solutions. In their study, the mass of oxygen incorporated into the electrode accounted for only 20-30% of the frequency changes they observed upon oxidation of the gold. Scanning electron microscopic (SEM) investigation on the electrodes revealed significant roughening of the surface upon oxidation, while the reduced surfaces were smooth. If the depth of the "pockets" in the oxidized films are no greater than a few angstroms, the solvent trapped in them will behave as a rigid layer. The increased mass of the oxidized electrode was therefore due to the incorporation of solvent into the "pockets" on the electrode surface.

The requirement of film uniformity also has a significant impact upon film deposition and dissolution studies, as was found by Ostrom and Buttry.<sup>70</sup> In their study of the deposition and dissolution mechanisms of diheptylviologen bromide films, frequency increases associated with film dissolution at higher voltammetric scan rates (cyclic voltammetry) occurred abruptly toward the end of the scans, while the frequency increases for dissolution at lower scan rates were gradual. They showed

that film dissolution at fast scan rates occurred by a pitting mechanism with the pits growing together over time. This resulted in film disintegration later in the scan for dissolution at higher scan rates (than for dissolution at lower scan rates). When the pits in the dissolving film were filled with solvent that had a density close to that of the film, the frequency increase due to film dissolution could not occur until the latter stages of disintegration for much the same reason as observed in Schumacher's study. At high scan rates, the frequency increases could not occur until solvent came into contact with the crystal surface.

Another factor affecting film uniformity is film porosity and swelling effects. Solvent incorporation into porous films can greatly affect their densities, shear moduli, viscosities, and thicknesses (due to swelling). For meaningful mass measurements to be made on such films, they must be thick enough (ca. 0.1  $\mu\text{m}$  or greater) to make surface roughness effects negligible. In a recent contribution, Borjas and Buttry<sup>76</sup> evaluated the effect of solvent swelling on the electrochemical behavior and stability of poly(nitrostyrene) (PNS) films in acetonitrile using the EQCM and conductance measurements. For PNS films, extensive solvent swelling adversely affected film stability. The additional viscous loading in such films due to solvent incorporation can be significant, as was observed by Lasky, Meyer, and Buttry<sup>71</sup>. In this work, to

be discussed in detail later, solvent incorporation into sensor polymeric films on the QCM resulted in mass changes significantly higher than expected, due to the reasons listed above. These effects are expected, however, in light of Kanazawa's work ( $Q_1$  functions).<sup>65</sup>

### 3. Stress Effects

In addition to stress effects placed upon the crystal by mounting structures, surface films can induce large stresses upon the QCM crystal. Ullevig, *et al*<sup>43</sup>, in a study of highly stressed Fe-Ni and Ni films on silver electrodes, found that the radial (mass) sensitivity function of the QCM crystal was drastically altered by the presence of these films. For the Fe-Ni and Ni films, the sensitivity was greater in the center of the crystal but that it dropped off much faster, compared to the crystal with silver electrodes only.

### F. Applications

The QCM has been successfully applied to a wide variety of problems. Some of the major applications are listed in Table 1 to give the reader an idea of the scope of the technique.

### G. Conclusion

From the above discussion, it can readily be seen that

<u>QCM Application</u>	<u>Researcher</u>
H <sub>2</sub> O vapor detector for Mars probe	King <sup>77</sup> , 1964-5
GC detector	Karasek <sup>78</sup> , 1974
LC detector	Konash <sup>57</sup> , 1980
thermogravimetric analyzer	Henderson <sup>79</sup> , 1982
determination of iodide in solution	Nomura <sup>80</sup> , 1982
NH <sub>3</sub> gas detector	Guilbault <sup>81</sup> , 1975
solution density, viscosity	Nomura <sup>82</sup> , 1982
chemical warfare agent sensors	Guilbault <sup>83</sup> , 1987
liquid phase adsorption isotherms	Lindstrom <sup>84</sup> , 1987
weighing monolayers of colloidal SiO <sub>2</sub>	Nordin <sup>85</sup> , 1988
study polystyrene surface swelling	Kramer <sup>86</sup> , 1990

Table 2.1 Some applications of the quartz crystal microbalance. Listed beside the application is a primary developer of the application and the year of the development. Additional applications are contained in a fine review by Guilbault.<sup>87</sup>

the QCM is a powerful tool with many possible applications. As with most "new" analytical techniques, there are limitations, but continuing research efforts are minimizing these. Its use in EQCM studies has given significant new insights into surface phenomena and processes, making it an extremely important new tool in physical chemistry studies. Its use as a basis for sensors is possibly one of the most technologically significant and far-reaching applications, however. As theoretical foundations for QCM use are extended, widespread routine use can be expected.

## CHAPTER III

### Quartz Crystal Microbalance Studies of Solvent and Ion Uptake and Release in Poly(vinyl) Chloride Ion-Selective Electrode Films

#### A. Introduction

When a thin (several monolayers maximum) rigid film is attached to a crystal, it becomes a part of the oscillator ensemble. Since damping of the resonant oscillation does not occur, mass detection by the oscillator is governed by the Sauerbrey equation (equation 2.8), which can also be written as

$$\delta f = -f_0^2 m/N d = -2nf_0^2 m/[(d \mu)^{1/2}] \quad (3.1)$$

where  $N$  is the frequency constant of the quartz crystal used ( $N = 0.167 \times 10^6$  Hz cm),  $d$  is the density of the quartz ( $2.648$  g/cm<sup>3</sup>),  $\mu$  is the shear modulus of quartz ( $\mu = 2.947 \times 10^{11}$  g/cm s<sup>2</sup>), and  $n$  is the number of the harmonic at which the crystal is being driven (i.e. 1 for the fundamental, 3 for the third harmonic, etc.). For 5 MHz AT-cut crystals as used in this study, Sauerbrey's equation can be written as

$$\delta f = -C_f \delta m \quad (3.2)$$



where  $C_f$ , the mass sensitivity coefficient, is 56.6 Hz  $\mu\text{g}/\text{cm}^2$ . In accordance with this relationship, as mass is deposited on the oscillator surface, the resonant frequency of the crystal will decrease. Studies on the underpotential deposition of various metals<sup>88</sup> and solvent and ion incorporation in rigid films<sup>89</sup> yielding absolute mass changes are exemplary of the mass sensing capacity of the QCM in solution.

If the attached films are too thick or are not rigid, acoustic losses can occur since the surface shear wave would be progressively damped as it travels through such films. Solvent swollen polymeric films such as those used in this study frequently exhibit such (viscoelastic) damping effects. Although the relative magnitude of these effects can be ascertained by impedance analysis, adherence to the Sauerbrey equation is no longer observed since the viscosity, shear modulus, density, and thickness of the film must now be considered in the calculations, as was discussed earlier.<sup>65</sup>

If linear plots of the frequency change versus concentration of the analyte (concentration profiles) can be obtained for such films, their utility in a QCM-based sensor would be established. Lasky and Buttry's glucose sensor using viscoelastic cross-linked polyacrylamide films as a matrix meets this requirement.<sup>36</sup> Adherence to the Sauerbrey equation is therefore not a requirement for use

of the QCM as an analytical mass sensor. Although the development of a QCM-based ionic sensor using these films was not a goal of this study, the partial satisfying of this requirement provided additional support for the findings (detailed below).

Since mass (ions and solvent) is incorporated into and expelled from PVC-based ISE sensor films during their operation, the QCM is ideally suited to study ion and solvent uptake and release processes in these systems. Because the films are viscoelastic and changes in their viscoelasticity are expected to take place *during the course of an experiment*, application of the Sauerbrey equation to reveal the absolute mass changes involved in these processes is ruled out. This does not, however, negate the utility of the QCM in this study. That changes in the films' viscoelasticity occur during these processes is in itself proof that solvent is incorporated into the films during sensor operation (see below).

In this study, a typical experiment would involve flowing solvent blank (water) and test solutions through a flow cell containing a crystal coated with a PVC ISE-type membrane. Since studies<sup>2,22</sup> have established that water is taken up by PVC membranes, solvent blank is first flowed into the cell to allow hydration of the PVC membrane. The frequency decreases considerably during this process (ca. 1500 Hz). Once the membrane is hydrated, as evidenced by

stabilization of the frequency response (referred to as the solvent saturated frequency value), the test solutions can be flowed into the cell.

When a test solution reaches the membrane, the analyte cation is complexed by the membrane-bound (hydrophobic) ionophore at the membrane-solution interface and pulled into the membrane. Waters of hydration associated with the analyte cations may also accompany them into the membrane. The net result is an increase in the mass attached to the crystal's surface, and the resonant frequency of the crystal should therefore decrease. When solvent blank is flowed back into the cell, the membrane-bound cations partition back into the solvent, and any water that entered the membrane with them should leave as well due to solubility considerations. The frequency change associated with this process should be equal to the change occurring during ion and solvent incorporation, and the oscillation frequency of the QCM crystal should return to the solvent saturated frequency value. A frequency versus time trace for such an experimental cycle is shown in Figure 3.1. Analyte concentration changes should result in proportionately different frequency responses, as well.

In studying Figure 3.1, it is important to note the time required for an experimental cycle. As compared to ISEs with response times of less than 30 seconds, the response time for most of the films in this study was 5-7

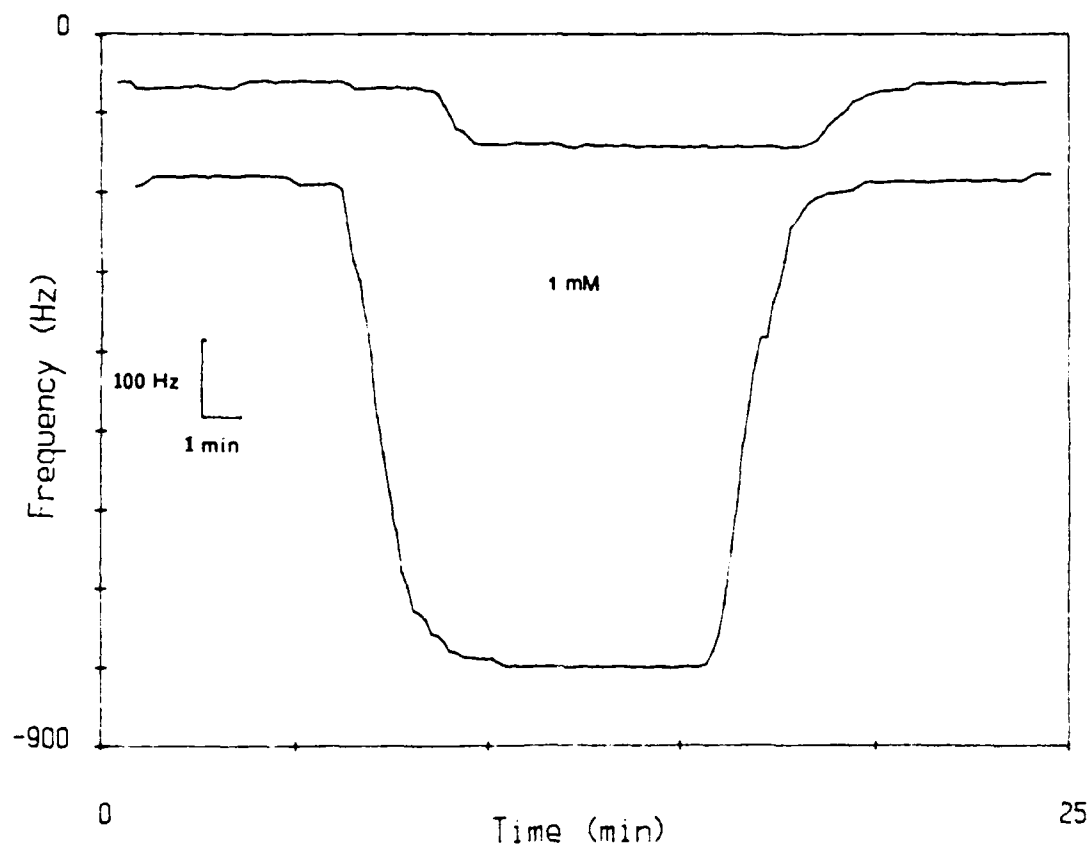


Figure 3.1 Frequency versus time trace for an experimental cycle. Top trace: reference film response. Bottom trace: sensor film response.

minutes, as measured from the instant the analyte solution flow was started to the point where the frequency change stopped (see Figure 3.1). The time required for one full experimental cycle was typically 20-30 minutes because of this. That solvent and ion uptake by the reference films (see Chapter 1) is considerably less than that for sensor films is easily seen here, as well.

Since the film properties change due to solvent and ion incorporation and expulsion during such a cycle, the conductance spectra for the films at different times in an experimental cycle should vary significantly. The film thickness and  $Q_1$  values may also vary as well. The situation encountered in such an experiment is therefore expected to be extremely complex, and several analytical techniques will have to be employed to elucidate the relevant events occurring in these films.

#### B. Experimental

5 MHz AT cut, overtone polished, quartz crystals (Valpey-Fisher) are coated as follows. The crystals are silanized with 3-mercaptopropyltrimethoxysilane (M8500, Petrarch) in  $\text{CH}_2\text{Cl}_2$  (Baker) to provide a substrate (approximately 1 monolayer) to which the gold can adhere. Gold (99.9%, D.F. Gold-smith) "keyhole" electrodes are then vapor deposited onto the silanized crystal in an Edwards E306A coating system to give electrodes of approximately

300nm thickness. The crystals are then resilanized with octadecyltrichlorosilane (09750, Petrarch) to cap the pendant mercapto groups not covered by gold, making the entire crystal surface hydrophobic. A diagram showing a coated crystal is illustrated in Figure 3.2. The central area of the crystal sandwiched between the gold pads ( $0.28 \text{ cm}^2$ ) is the piezoelectrically active area.

PVC membrane stock solutions were prepared using PVC (Fluka Selectophore HMW or Aldrich HMW) and dioctyl sebacate (DOS, Aldrich), dioctyl adipate (DOA, Aldrich) or o-nitrophenyloctyl ether (o-NPOE, Fluka) as the plasticizer. Tetrahydrofuran (THF, Burdick and Jackson) was used as the solvent. The sensing species used were dibenzo-18-crown-6 (termed CE; Aldrich), a potassium ionophore, and bis[(12-crown-4)-2-ylmethyl]-2-dodecyl-2-methyl malonate (referred to as bisCE; Sigma), a sodium ionophore. These ionophores are shown in Figure 3.3. The final membrane concentrations for all the membranes (unless otherwise noted) were; reference - 43.4% PVC, 56.6% plasticizer; sensor - 42.8% PVC, 56.0% plasticizer, 1.2% ionophore. Except where noted, all of the membranes were prepared using CE as the ionophore. Higher ionophore concentrations were used in some films, and results for such films are annotated with the ionophore concentration for ease of reference.

The PVC ISE-type membranes are cast on the gold pad of the crystal by drop evaporation. Although this resulted in

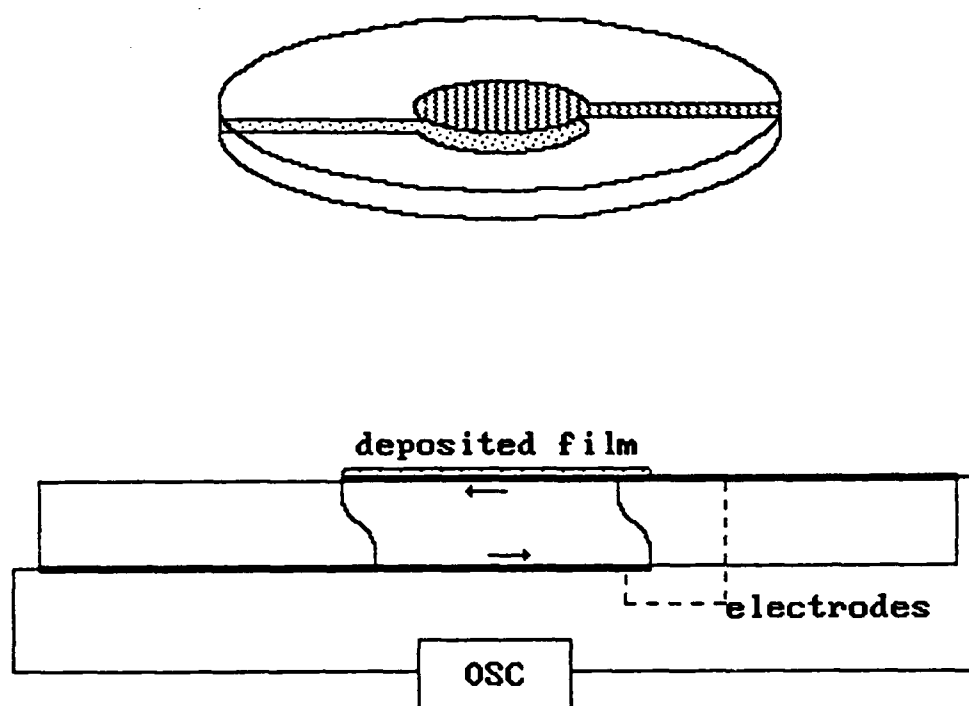


Figure 3.2 Top: 5 MHz AT-cut crystal similar to those used in this study. Bottom: Diagram of a PVC film attached to the electrode surface on the crystal.

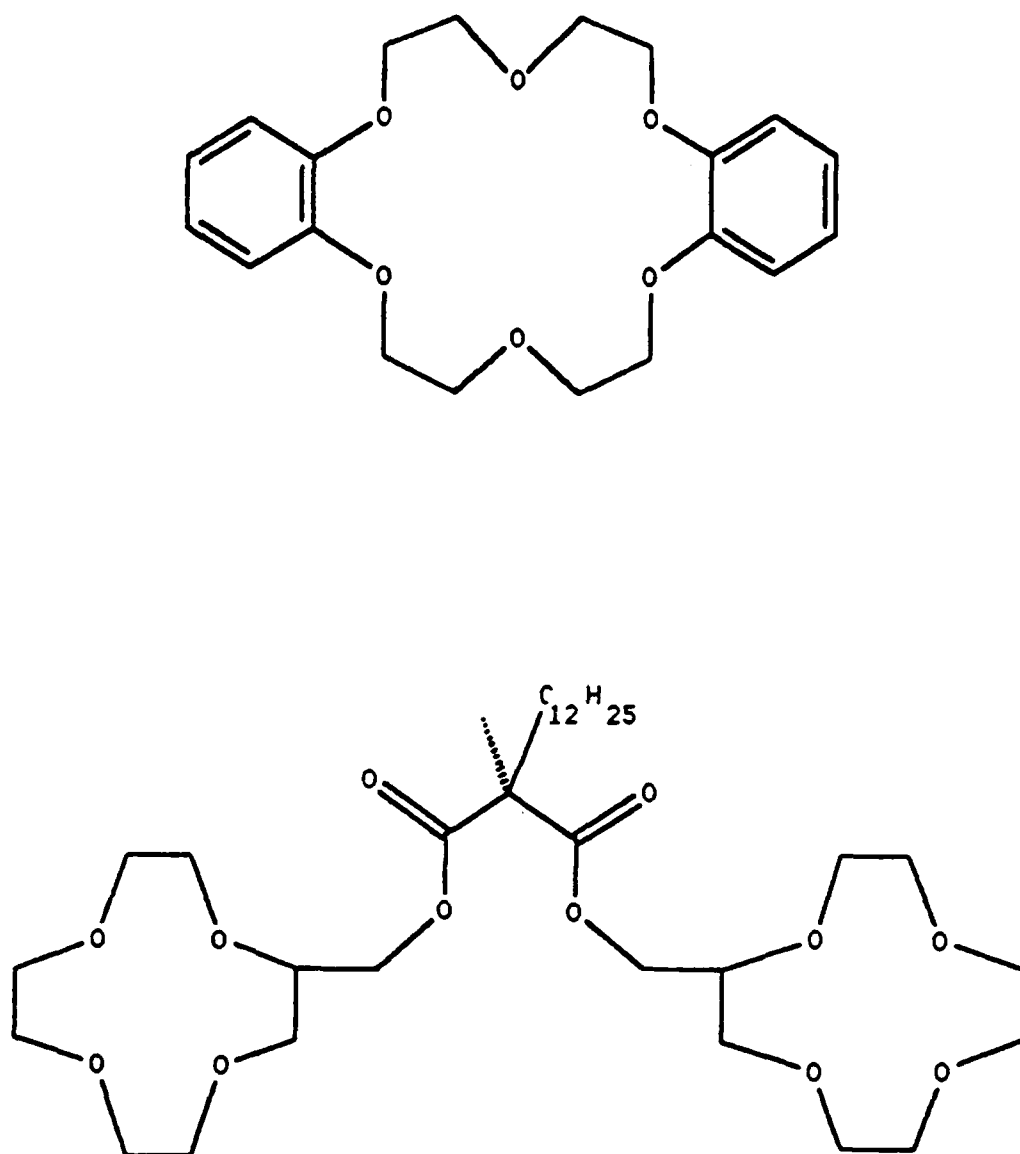


Figure 3.3 The ionophores used in this study.

Top: Dibenzo-18-crown-6, a potassium ionophore.

Bottom: Bis[(12-crown-4)-2-ylmethyl]-2-dodecyl-2-methyl malonate, a sodium ionophore.



visibly nonuniform membranes (surfaces rippled), it was the only method tried that resulted in operable membranes. Other techniques of film casting which were attempted included spin coating (by far the worst method) and drop evaporation in a THF saturated atmosphere. Membranes produced by the latter method were very uniform, but had very short lifetimes (<30 min). This is most likely due to concentration of the ionophores at the membrane surface during THF evaporation, since these species are more soluble in THF than in the PVC/plasticizer matrix. When these membranes were exposed to analyte solutions, loss of the ionophore from the membranes into solution (an expected phenomenon<sup>33</sup>) occurred much more quickly than for drop evaporation cast membranes. Dip coating was not tried since the amount of ionophore required to make the dip solutions would have been excessive.

Film thickness measurements were made using a Rudolph Research AutoEL ellipsometer. Impedance spectra were obtained using a HP4192A LF Impedance Analyzer interfaced to a IBM PC-AT, using the ASYST programming environment. It is these measurements that allow one to detect the effects of viscoelastic damping on the crystal oscillator.

Frequency response measurements for the films were made in a differential mode using two crystals in a flow cell (Figure 3.4). A reference crystal is placed in one side of the flow cell and a sensor crystal in the other side.

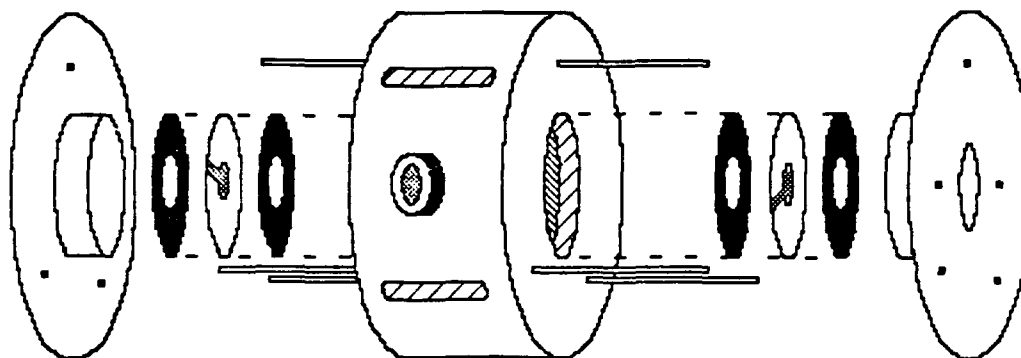


Figure 3.4 Flow cell used in the experiments. The reference crystal goes in one compartment and the sensor crystal goes in the other. Electrical contact is made with clips attached to the crystals through the oblong access ports on the sides of the cell.

Differential measuring allows one to subtract out any mass changes due to solvent and ionic uptake by the films due to the PVC alone. This is necessary because PVC is expected to hydrate in water<sup>2,22</sup> and PVC has been shown to be a low capacity ion-exchanger<sup>20,90</sup>. It is assumed that these effects are the same for both membranes since their compositions are almost identical. The magnitude of these effects is also considerably smaller than those due to incorporation of ions and associated solvent into the sensor films, as will be seen later.

The experimental set-up is shown in Figure 3.5. Flow rate of the analyte solutions through the cell (3.7mL/min) was controlled with a Wiz RP pump. Frequency measurements were made with a Philips PM6654 frequency counter and recorded on a Kip and Zonen BD91 XYY' recorder with the X-axis being time-based. All frequency measurements were made at room temperature.

All solutions (analyte and solvent blank) used with CE membranes were saturated in CE to hinder carrier loss from the already thin sensor films. Reagent grade (or higher) salts were used. All reagents were used as obtained without further purification. CE-K<sup>+</sup> complex concentrations for the salt solutions were estimated using the solubility data for the CE in water at 26 +/- 5°C.<sup>9</sup>

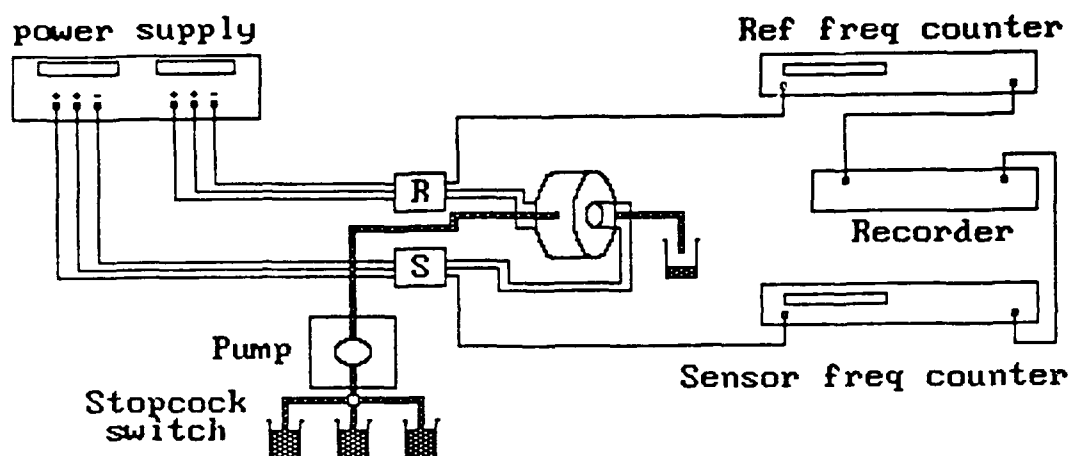


Figure 3.5 Experimental set-up. R, S = Reference and sensor oscillator circuits. These circuits are powered by an HP6205C power supply. The solutions are pumped through the cell at a rate of 3.7 mL/min by a Wiz RP pump. Frequency measurements are made on Philips 6654 frequency counters and recorded on a Kipp and Zonen BD91 (XY'Y') recorder.

## C. Results and Discussion

### 1. The Membranes

PVC was regarded as an inert matrix by most early PVC ISE researchers. With the exception of a study of the  $T_g$  (glass transition temperature) of plasticized PVC membranes in 1973 by Fiedler and Ruzicka,<sup>96</sup> very few studies on the properties of plasticized PVC and how they affected ISE operation were conducted. Recently, several papers addressing various aspects of this topic have appeared.<sup>7-9,14,23,30,90,92,97</sup> The overall results from these studies are as follows.

PVC ISEs contain impurities that act as ion exchange sites during membrane operation<sup>23</sup>. These sites are relatively immobile, and are thought to contain sulfur species (e.g.  $SO_3^{2-}$ )<sup>30,97</sup> that are believed to be precursors (initiators) in the PVC manufacturing process. The concentration of such sites in plasticized 33% PVC ISE membranes is estimated at 0.05-0.6mM,<sup>23</sup> making these membranes low capacity ion exchangers.<sup>90</sup> PVC is also responsible for the formation of solvent-separated ion pairs within the membranes<sup>8</sup>. That the membranes take up water during operation has been proposed for over ten years,<sup>17</sup> and is confirmed in this study (see below). However, a study quantifying the amount of water in the membranes has not yet appeared.

Since the purpose of this study was to examine ion and solvent uptake into and release from PVC-based ISE-type membranes during operation, membranes of the classical PVC ISE formulation (33% PVC, 66% plasticizer, and 1% neutral carrier) were tried first. Unfortunately, these films hydrated so extensively that delamination from the crystal occurred in almost all cases (verified by visual and optical microscopic inspections of the films), and usually within one hour. None of these films gave reproducible frequency changes for 1mM KCl solutions.

In an attempt to make the films more stable and have greater lifetimes, the concentration of PVC was increased to 43-45% (43% with o-NPOE and DOS and 45% with DOS and DOA). The resultant films were much more stable than the 33% PVC films. Many sets (reference and sensor) of these films gave linear responses to incremental analyte concentration changes. The ionic diffusional coefficients in these films, however, are expected to be at least an order of magnitude less (approximately  $10^{-9}$  cm<sup>2</sup>s<sup>-1</sup>) than for membranes containing 33% PVC since the dielectric constant of these membranes is greater.<sup>8,9,92</sup> These films, therefore, can only be used as models for PVC-based ISEs.

Three plasticizers (DOA, DOS, and o-NPOE) were used in the process of trying to get more stable films, as well. DOS and o-NPOE plasticized films were better, as expected, due to their higher lipophilicities and dielectric

constants.<sup>11,33,94-5</sup> Even though DOS and o-NPOE films were better, less than 30% of all these films had reproducible responses to the analyte or long enough lifetimes to be of use in this study. The observed frequency changes for films plasticized with o-NPOE were considerably less than those for films using DOS and DOA, however. This was not unexpected since the fact that different plasticizers can affect the sensitivity (as well as the selectivity) of neutral carrier ionophores was been reported by Thomas, *et al.*<sup>94</sup> and Attiyat, *et al.*<sup>95</sup> No further attempts at film optimization were made, since higher PVC concentrations would result in films too different from those used in PVC ISEs.

Higher ionophore concentrations (greater than 1%) were used with CE in preliminary tests, and larger responses to the analyte were observed, but the lifetimes of the membranes were still too short and they had constant, unacceptably large, frequency losses (uniform frequency decreases of ca. 1 Hz/min or greater). Higher ionophore concentrations were also used with bisCE in the last series of films studied (discussed below). A cursory study of vastly different PVC concentrations was conducted, with results summarized in Table 3.1.

Even with the 43-45% PVC concentration, membrane lifetime was generally 1-2 days at best. In a study of PVC/VAGH (vinyl chloride/vinyl alcohol copolymer) membranes

Table 3.1

Film composition vs. maximum response for 1mM KCl

<u>PVC %</u>	<u>Plasticizer %</u>	<u>Maximum response, Hz</u>
99	0	~70 <sup>1</sup>
80	19	~10
43	56	>1000
33	66	1000 <sup>2</sup>

<sup>1</sup>Nonlinear frequency versus concentration changes occurred here.

<sup>2</sup>The lifetimes of these membranes were too short to be of value.



for an ion selective field effect transistor (ISFET) sensor, Moody, et al,<sup>96</sup> found that as the thickness of the membranes was decreased from 150 $\mu$ m to 50 $\mu$ m, the membrane lifetimes dropped from greater than 28 days (the membranes were discarded at that point) to as short as 8 days. They hypothesized that ionophore loss from the membranes was the primary cause for the observed decrease in membrane lifetimes. Ionophore loss was also noted by Thomas, et al,<sup>16</sup> and Oesch and Simon<sup>33</sup> in their studies of ionophore and plasticizer effects on PVC ISE membrane performance. Thomas<sup>7,93</sup> has written on these effects in two recent reviews. Since some CE was expected to partition into the solvent blank and analyte solutions because of its solubility in water (see below), a second ionophore, bis[(12-crown-4)-2-ylmethyl]-2-dodecyl-2-methyl malonate, bisCE, was tried. This ionophore has a greater lipophilicity *and* a greater specificity for the analyte ( $\text{Na}^+$ )<sup>98</sup> than CE. The success rate (for producing usable membranes) with this ionophore was considerably greater than with CE.

Plasticizer loss from the membranes into the contacting solutions can also occur, as was noted by Oesch and Simon<sup>33</sup> in the most thorough study of ionophore and plasticizer effects on PVC ISE membrane lifetimes to yet appear. Although plasticizer loss from the membranes used in this study is possible, this mechanism of membrane

degradation is thought to be less important because the plasticizers are viscous and quite hydrophobic. However, since the membranes in this study are 2-3 orders of magnitude thinner than normal PVC ISE membranes and solvent swelling of the membranes is significant (see below), this mechanism cannot be neglected, and will be discussed later.

## 2. The Solutions

In the present study, one of the two ionophores used, dibenzo-18-crown-6 (CE), is considerably more soluble in water than the ionophores used in Thomas' and Oesch and Simon's studies. CE should therefore partition into the solution as CE-(analyte ion)<sup>+</sup> complexes or free CE, adversely affecting membrane lifetimes and responses to analyte solutions. Since the membranes used in this study are 2-3 orders of magnitude thinner than "normal" PVC ISE membranes, ionophore loss from the films would have a significant effect on their performance. These phenomena (membrane thickness and ionophore solubility) are the major factors to which the observed short membrane lifetimes can be attributed. By saturating all the solutions used with these membranes with CE, the partitioning process should have been hindered. That sensor (CE) membranes used with these CE saturated solutions had longer lifetimes than those used with normal solutions (no CE added) empirically confirms this hypothesis. Even with these solutions being

saturated in CE, however, the predominant species involved in membrane interactions were the analyte cations because CE-analyte<sup>+</sup> concentrations in the solutions were 1.5-2.5 orders of magnitude less than the lowest salt concentrations used.<sup>91</sup>

### 3. Membrane Responses

As mentioned in the Experimental section, all the frequency measurements were made in a differential mode. Reference membranes containing no ionophore were used so solvent and ion uptake by the films due to the ion-exchanging abilities of PVC could be accounted for. All the reported frequency responses are actually net (sensor minus reference) responses, as shown in Figure 3.1, which illustrated the experimental response of reference and sensor films to solvent blank (CE saturated water) and an analyte solution (CE saturated 1mM KCl).

Based upon the amount of ionophore incorporated into the sensor films during fabrication, the frequency change calculated from the Sauerbrey equation for saturation of all carrier sites in the 1% CE membranes with K<sup>+</sup> is 9 Hz. The theoretical responses for other membranes used in this study are listed in Table 3.2. The only factors that could make the observed frequency changes higher than this are solvent uptake by the membranes and viscoelastic damping effects in the films since the differential measuring

Table 3.2

Theoretical Versus Actual Responses for Various Membrane Formulations<sup>1</sup>

<u>PVC%<sup>2</sup></u>	<u>Plasticizer%</u>	<u>Ionophore%</u>	<u>Theor. Resp.</u>	<u>Act. Resp.</u>
40.9% #1	58.9% DOA	1.2% CE	~10 Hz	1050 Hz
40.9% #2	58.9% DOA	1.2% CE	~10 Hz	365 Hz
39.8% #2	59.4% o-NPOE	1.1% CE	~10 Hz	33 Hz <sup>3</sup>
42.8% #2	55.9% DOS	1.2% CE	~10 Hz	140 Hz
40.6% #2	53.0% DOS	6.4% bisCE		~4000 Hz
40.6% #2	53.0% DOS	6.4% bisCE		~4000 Hz <sup>3</sup>

<sup>1</sup>Theoretical response is calculated for saturation of all membrane ionophore sites with analyte ions. Actual responses are the membrane response to 1mM analyte solutions.

<sup>2</sup>For PVC types , #1 = Aldrich HMW PVC and #2 = Fluka Selectophore PVC.

<sup>3</sup>These membranes were 1.5 $\mu$ m thick. All other membranes were 1.3 $\mu$ m thick.

scheme minimizes other possible film effects. Since the observed frequency responses are much greater than this, as seen in Figure 3.6 and Table 3.2, solvent incorporation into the films during sensor operation is suspected to occur.

Concentration profiles were run on several sets of films. The observed frequency changes were nearly linear as a function of analyte concentration. This is expected in light of the analytical utility of PVC-based ISEs, although for quite different reasons. The response of an ISE to an analyte ion is governed by the Nikolskij-Eisenman equation (in the presence of interfering species), which has a logarithmic relationship between analyte concentration and sensor response, as evident in equation 3.3.

$$E = RT/z_1 F \left[ \ln \left( a_1 + \sum K_{1j} a_j^{z_1/z_j} \right) \right] \quad (3.3)$$

The response for these QCM-based sensors should be linear with concentration since more ions (and solvent) will enter the films while sensing higher concentration analyte solutions. Response times for the QCM-based sensors is much longer because a mass equilibrium must be established, and as pointed out earlier, the diffusion coefficients of the ions in these membranes is  $10^{-9} \text{cm}^2 \text{s}^{-1}$  or less and the membranes are ca.  $1.5 \mu\text{m}$  thick. While these experiments are hours long, similar experiments using ISEs (electrochemical sensing mode) would take a few minutes at most. Typical

**Figure 3.6 A typical (KCl) concentration profile for a 2.2 $\mu$ L thick 1.2% CE film set. Top trace: reference film response. Bottom trace: sensor film response.**

concentration profiles are shown in Figure 3.6.

The frequency responses for "good" membranes varied with time, as shown in Table 3.3. The method of membrane storage between use appeared to be the major factor affecting the membrane responses for membranes that lasted longer than two days. Storage method also affected the lifetime of these membranes as well. CE membranes stored in KCl (CE saturated) solutions had, by far, the shortest lifetimes, but storage in these solutions improved membrane response, as shown in Table 3.3. This was expected, as ISEs are stored in salt (halide) solutions of the analyte ion to increase their sensitivity. CE loss during storage in these solutions would be greatest, however, since  $K^+$  partitioning between the membranes and solution (with concurrent loss of CE and/or CE- $K^+$  complexes from the membranes) would also occur in the thin membranes used in this study. The CE membranes having the longest lifetimes were stored in water (CE saturated) or dry. The bisCE membranes were stored in water or dry. Storage effects on membrane lifetime for both sensor ISE were not quantified, however.

As mentioned earlier, film uniformity can have an effect on the observed frequency changes. Although the surfaces of the films were visibly rippled, the variation in film thickness (across a film) was less than 10% as measured ellipsometrically. This could account for some

Table 3.3

Summary of frequency responses (in Hz) vs membrane  
lifetime<sup>1</sup>

<u>KCl conc, mM</u>	<u>day 1</u>	<u>day 2</u>	<u>day 3</u>	<u>day 4<sup>2</sup></u>	<u>day 5</u>	<u>day 6</u>
.1	49	43	41	48	40	32
.5	215	211	176	235	205	183
1	407	398	362	485	411	355
3	---	784	---	1050	---	---

<sup>1</sup>Day 1 - day 6 cover a period of almost two weeks. Most of the measurements shown here were taken at least two days apart.

<sup>2</sup>Responses after soaking for 2.5 days in ~1.5 mM KCl.



variation in frequency responses between the reference and sensor crystals, but since this was beyond experimental control and could not be quantified experimentally or theoretically, its presence was tolerated.

#### 4. Conductance Studies

Conductance spectra were obtained for the membranes in dry, solvent-wetted, and analyte-wetted states to gain insight into the changes occurring in the membranes during an experimental cycle. The important values to note in the conductance spectra are the resonant frequency,  $F_0$ , and the  $\Delta F$ , full width half maximum (FWHM), values. Mass loss or gain by the membranes would result in  $F_0$  changes (mass loss resulting in a frequency increase), while membrane viscoelastic changes would be reflected in both the  $\Delta F$  values (the more rigid a membrane, the smaller its  $\Delta F$ ) and  $F_0$  changes (due to viscous losses in the membranes).

During solvent uptake (with or without concurrent ionic uptake) by the membranes, the shear modulus and density of the membranes would decrease while their viscosity and thickness (due to swelling) will increase. These effects result in increases in the  $\Delta F$  values and decreases in the  $F_0$  values. Solvent and ionic uptake (mass gain) would also cause  $F_0$  (frequency) drops. The large frequency drops and  $\Delta F$  increases observed upon going from a dry to a solvent-wetted condition imply that

hydration is occurring in both reference and sensor membranes. The additional frequency drops and  $\Delta F$  increases upon going from solvent-wetted to analyte-wetted states imply that further solvent uptake occurs during cation incorporation. It is important to note that as the membranes swell, surface pore sizes will also increase. This means that as the analyte concentrations are linearly increased (as in a concentration profile experiment), the membrane swelling (with concurrent pore size increases) will allow *greater than linear* increases in the amount of solvent entering the membranes with analyte ions. Some of the solvent entering the membranes is expected to be associated with the analyte ions, however, most of the solvent thus entering the membrane is thought to be unassociated (free) solvent.

As ions and solvent are incorporated in the CE membranes from 1mM KCl solutions (CE saturated), the  $\Delta F$  values change. The magnitude of these changes with 1mM KCl, however, is small in comparison to the original  $\Delta F$  values, as seen in Table 3.4. This is important because it implies that viscoelastic changes in the membrane during the course of an experiment (due to solvent and ion uptake by the membranes) have little effect on the observed  $F_0$  changes. The  $\Delta F$  change on going to higher analyte solution concentrations, however, is expected to become greater as more solvent can enter the membranes due to

Table 3.4

Conductance ( $F_0$  and  $\Delta F$ ) Values for Membranes

<u>Membrane</u>	<u>State</u>	<u><math>F_0</math> (Hz)</u>	<u><math>\Delta F^1</math> (Hz)</u>
Reference	dry	5004640	1460
	solvent	5003599	3540
	1mM KCl	5003459	3660
Sensor	dry	5025040	1980
	solvent	5024160	3960
	1mM KCl	5023459	4020

<sup>1</sup> $\Delta F$  values for dry *rigid* membranes are typically 40-80 Hz.

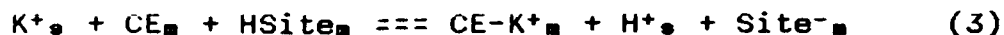
greater as more solvent can enter the membranes due to increased membrane pore size.

The effects of solvent and ion uptake on conductance spectral  $F_0$  and  $\Delta F$  for a sensor membrane can be seen in Figure 3.7. Table 3.4 shows  $F_0$  and  $\Delta F$  values for reference and sensor membranes in all three of the mentioned states. The effects mentioned above can be clearly seen here for both sensor and reference membranes.

## 5. Membrane Sensor Evaluation

### a. Charge Balance and Donnan Failure

As analyte cations are complexed at the membrane's boundary and enter the membrane, protons, thought to be due to acidic organic precursors in the PVC from its time of manufacture,<sup>23,30</sup> leave the membrane to maintain electroneutrality. It is the presence of these organic "impurities" that makes PVC a low-capacity ion-exchanger.<sup>90</sup> The analyte cations are thus associated with the resulting anionic sites, although the analyte cation-membrane site ion pairs are solvent separated.<sup>9</sup> The relationship below summarizes this process.



The "s" and "m" subscripts refer to solution and membranic species.

Donnan exclusion occurs as long as anionic sites are produced. Since the ionophore concentration (>1%) is much

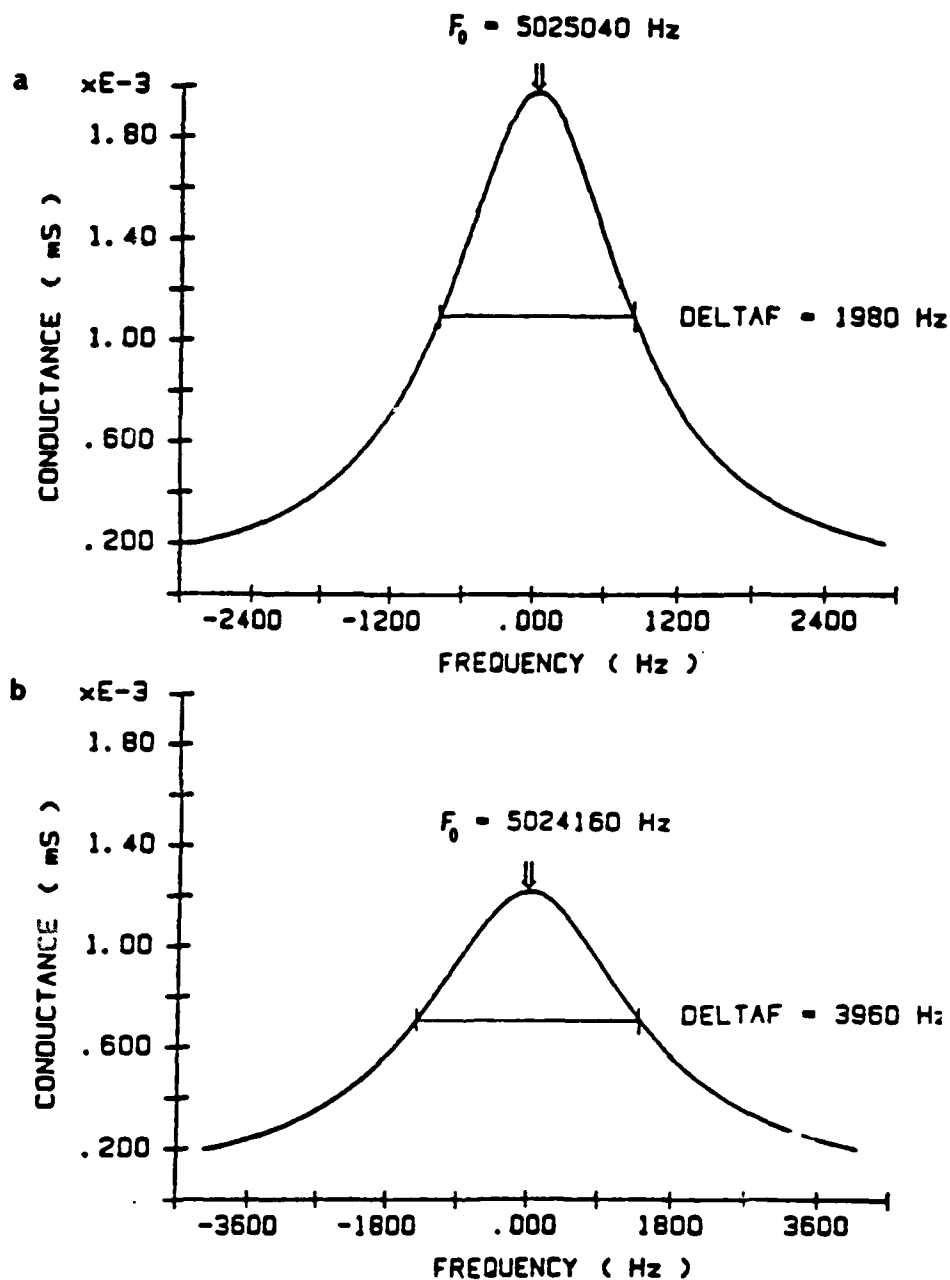


Figure 3.7 Conductance spectra for sensor membranes.  
a. Dry membrane. b. Sensor membrane in water (CE saturated). Note the frequency decrease and spectral broadening in the solvent saturated membrane.

larger than the site concentration, Donnan failure should occur if the analyte concentration is high enough to produce ionophore-analyte complex concentrations greater than the membrane site concentration. At this point, analyte ions will continue to enter the membrane (along with solvent) since free ionophore molecules are still present in the membrane. Because the site concentration is depleted, however, co-ions from solution must now enter the membrane to maintain electroneutrality (Donnan failure). Additional water (associated with the co-ions) would also enter the membrane well.

Figure 3.8 shows visually the onset and final result of Donnan failure in a CE sensor membrane induced by increasing analyte concentration. Since the concentration of sites in the membrane is less than the CE concentration (see above), co-ion insertion into the membrane must occur to maintain electroneutrality as more analyte enters the membrane. Up to this point, nearly linear frequency responses with increasing analyte concentration are observed. As the site saturation limit is approached, however, the differential changes become progressively less with increasing analyte concentration. This situation parallels the potentiometric response plateau that occurs in ISEs as Donnan failure occurs. In Figure 3.8, this effect becomes noticeable above 2mM. For further  $K^+$  uptake to occur in this sensor film, anions must also enter

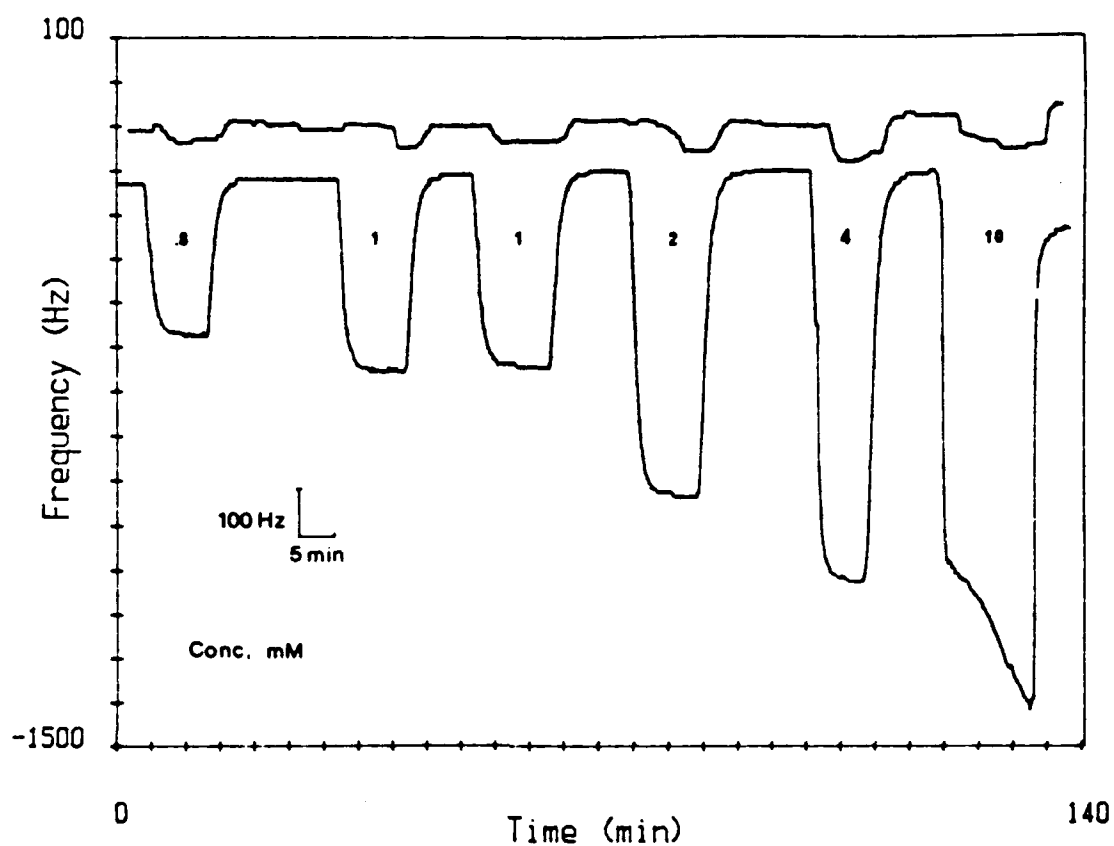


Figure 3.8 KCl Concentration profile for a CE sensor film showing site saturation and incipient Donnan failure. Note that this effect occurs only in the sensor membrane because there is no driving force present (i.e. ionophores) in the reference membrane to pull analyte ions in.

the membrane. Water (associated with  $\text{Cl}^-$  and  $\text{K}^+$  entering the membrane) continues to enter the membrane, and the observed frequency drop is now due to uptake of  $\text{K}^+$ ,  $\text{Cl}^-$ , and water. It is interesting to note that in the experiments where this phenomenon was observed, the rate of frequency drop after Donnan failure accelerated with time. No attempts to attain a maximum response (saturation of all CE sites in the membrane) were made.

#### b. Co-ion and Counter-ion Studies on CE Membranes

Experiments with different co-ions ( $[\text{Fe}(\text{CN})_6]^{3-}$ ,  $\text{Cl}^-$ ,  $\text{Br}^-$ ,  $\text{I}^-$ ) were done with the CE membranes to verify that the sensors were responding to  $\text{K}^+$  alone. Even in the case of ferricyanide, there were no significant differences in observed frequency changed, as can be seen in Table 3.5. These results verify the assertion that Donnan exclusion is occurring, because uptake of anions of different masses would result in different frequency responses for two  $\text{K}^+$  salt solutions of the same concentration but with different co-ions. Experiments with co-ions other than  $\text{Cl}^-$  in the limit of Donnan failure were not performed.

A cursory study with counter-ions resulted in significant differences in membrane responses, as is expected due to the different selectivities for the ions studied ( $\text{Na}^+$ ,  $\text{Li}^+$ ,  $\text{Cs}^+$ ,  $\text{Mg}^{2+}$ , and  $\text{Ca}^{2+}$ ). The results correlated fairly well with the reported selectivity



Table 3.5

Co-ion Responses (in Hz) for CE Sensor Membranes

<u>Conc., mM</u>	<u>KCl</u>	<u>KBr</u>	<u>KI</u>	<u>K<sub>3</sub>Fe(CN)<sub>6</sub></u>
.1	32	33	33	-
.5	183	184	167	396 <sup>i</sup>
1	355	357	350	512 <sup>i i</sup>
1.5	367 <sup>i</sup>	-	-	-
3	519 <sup>i i</sup>	-	-	-

i.ii KCl/K<sub>3</sub>Fe(CN)<sub>6</sub> results compared for equivalent K<sup>+</sup> concentrations. These experiments were done several days prior to the others.

coefficients ( $K_{ij}$ 's; for extraction of one ion,  $i$ , over an interfering ion,  $j$ ) for  $K^+$  versus other alkali ions, however, since the development of a QCM-based sensor using these membranes was only a secondary goal, these studies were not completed.

BisCE membranes with 2.4%, 6.4%, and 10.7% bisCE in the membrane were prepared and tried later in the study to attempt to increase sensor lifetimes. These membranes had significantly longer lifetimes than CE membranes and had good responses to analyte solutions as well. This was expected since bisCE is very hydrophobic (compared to CE), and its selectivity for the analyte ( $Na^+$ ) is much higher than CE's. BisCE membranes were plasticized with DOS only. Concentration profiles,  $D_2O$  studies (see below), and membrane thickness (conductance) studies were conducted on these membranes.

#### c. $D_2O$ Studies

To ascertain the absolute amount of water entering the membranes, an independent method must be used since the membranes are known to be viscoelastic.  $D_2O$  has been successfully used as a solvent for this purpose in several studies in this group.<sup>36,46,76,89</sup> Upon changing the contact solution from  $H_2O$  to  $D_2O$ , a 10% frequency decrease is expected with rigid films since  $D_2O$  is 10% heavier than  $H_2O$ . The problem with doing such an experiment with

viscoelastic membranes is that the membrane viscosity, shear modulus, and density are also changed upon going from  $H_2O$  to  $D_2O$ . By Kanazawa's results,<sup>65</sup> a membrane with a different  $Q_1$  value results. Thus, even though the membrane thickness should not vary during this solvent switch, the film response may vary significantly, as seen in Figure 2.11. Only a few responses for such an experiment were obtained, however, the resultant frequency changes were several times larger than the film response to 1mM analyte solutions, as seen in Table 3.6. For the reasons listed above, these measurements are of little value in this study since they give no insight into how much solvent enters the sensor membranes. Such measurements, however, would be of great value, in conjunction with membrane thickness measurements, in ascertaining the validity of Kanazawa's work.

#### D. Conclusions

From the trends observed with thin poly(vinyl chloride) ISE-type membranes, it is apparent that uptake of very large amounts of solvent (water) occurs during operation of these sensors. Both QCM and conductance measurements support this assertion. The quantity of solvent entering the membranes could not be ascertained by this study, however, because the complex relationships between the membrane properties (viscosities, densities,

Table 3.6

6.4% bisCE Sensor Film Responses to D<sub>2</sub>O and 0.1mM Na<sup>+</sup>

<u>Theor. Response<sup>1</sup></u>	<u>.1mM Na<sup>+</sup> Response</u>	<u>D<sub>2</sub>O Response</u>
~2 Hz	135 Hz	745 Hz
~2 Hz	129 Hz	660 Hz

<sup>1</sup>Responses are for 1.5 $\mu$ m thick membranes, using two different membranes.

shear moduli, and thicknesses) and QCM frequency responses, as proposed by Kanazawa,<sup>65</sup> change constantly during the course of an experiment. Although these relationships are strictly theoretical in nature, some of these effects, such as variations in film response for membranes of different thicknesses and excessively low oscillation frequencies for thinner (ca. 1.6 $\mu$ m) membranes, were observed during the course of this study. A thorough study of these effects will soon begin.

The implications for the "normal" (0.1 to 1 mm thick) PVC ISE membranes are that extensive solvent uptake can be expected to occur within the first several microns of membrane contacting the solution, and possibly much further into the membrane. In their most recent paper, Armstrong and Horvai<sup>92</sup> refer to a study by Armstrong and Johnson<sup>99</sup> ("in press") where the water content of fully saturated membranes was found to be 0.4% by weight (0.6M). The results of this study, when published, should corroborate the current work and previous assertions of the highly hydrated state of these membranes.

Since the membrane pore size increases due to solvent swelling, ionophore loss with concurrent sensitivity decreases can occur, as was noted in this and other studies.<sup>33,96</sup> Formation of a highly resistive exuded plasticizer region on the membrane surface, as proposed by Buck,<sup>23</sup> could be explained by this process as well. All

these results support the "three-region membrane" model, illustrated in Figure 3.9, as proposed by Kedem, Perry, and Bloch<sup>28</sup> and modified by Buck to include the surface "exuded plasticizer" region.<sup>23</sup>

That water is incorporated into PVC-based ISEs during operation is significant, in that it gives an explanation for potentiometric (permselectivity) failure of these ISEs in high ionic strength systems. Since significant hydration of (at least) the membrane boundary layers occurs, the polymeric matrix would become very swollen. As the mean pore diameter of the sensor membranes increases, the likelihood of electrolyte incorporation and ensuing Donnan failure in high ionic strength electrolytes also increases. That trace amounts of co-ions have been found in the membrane boundary regions<sup>17,25</sup> in electrodialysis experiments may also be attributed to this fact.

For the sensor membranes used in this study, the response to analyte solutions is illustrated in Figure 3.10. As shown in this picture, the reference membranes (plasticized PVC) respond to analyte ion concentration changes due to the impurities in the PVC. These impurities account for the low capacity ion-exchanging ability of PVC ISE-type membranes. In the sensor membranes, the ionophores "pull" analyte ions in, along with associated and free solvent, as explained above. The sensor membranes are thus more solvent swollen than the reference membranes.

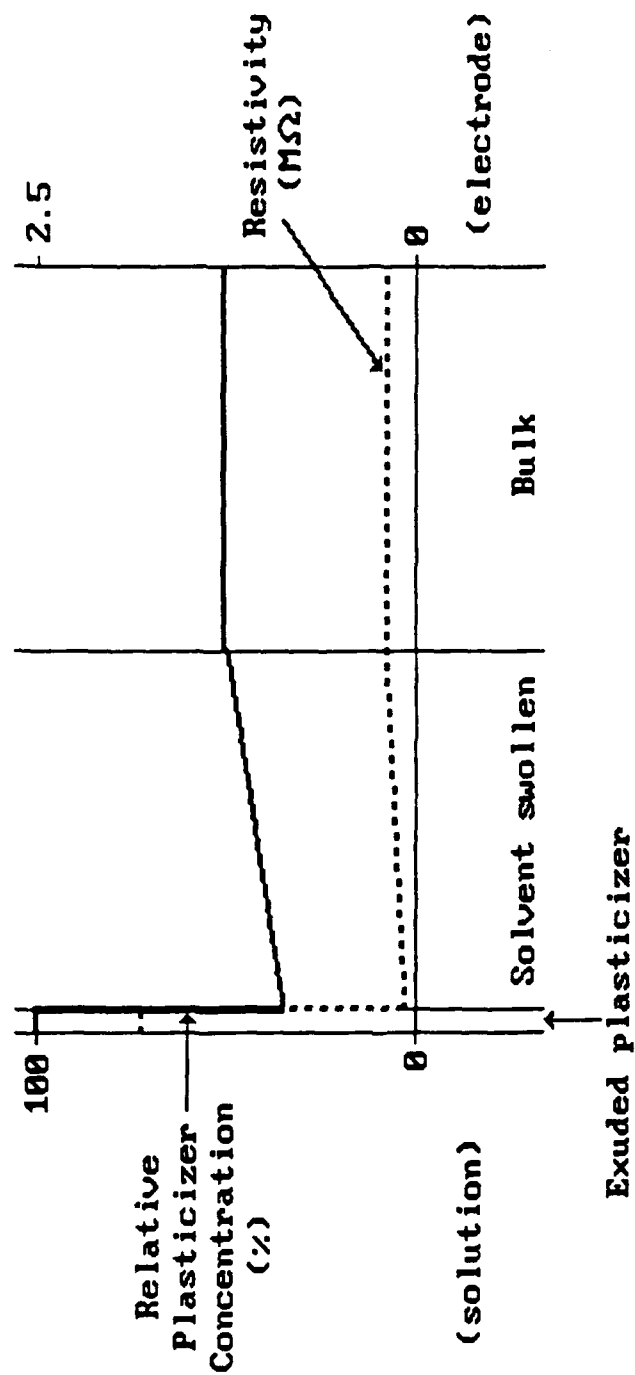


Figure 3.9 Figure illustrating the "three-region membrane" model. Relative plasticizer concentrations and region resistivities (as proposed by Buck<sup>23-25</sup>) are shown.

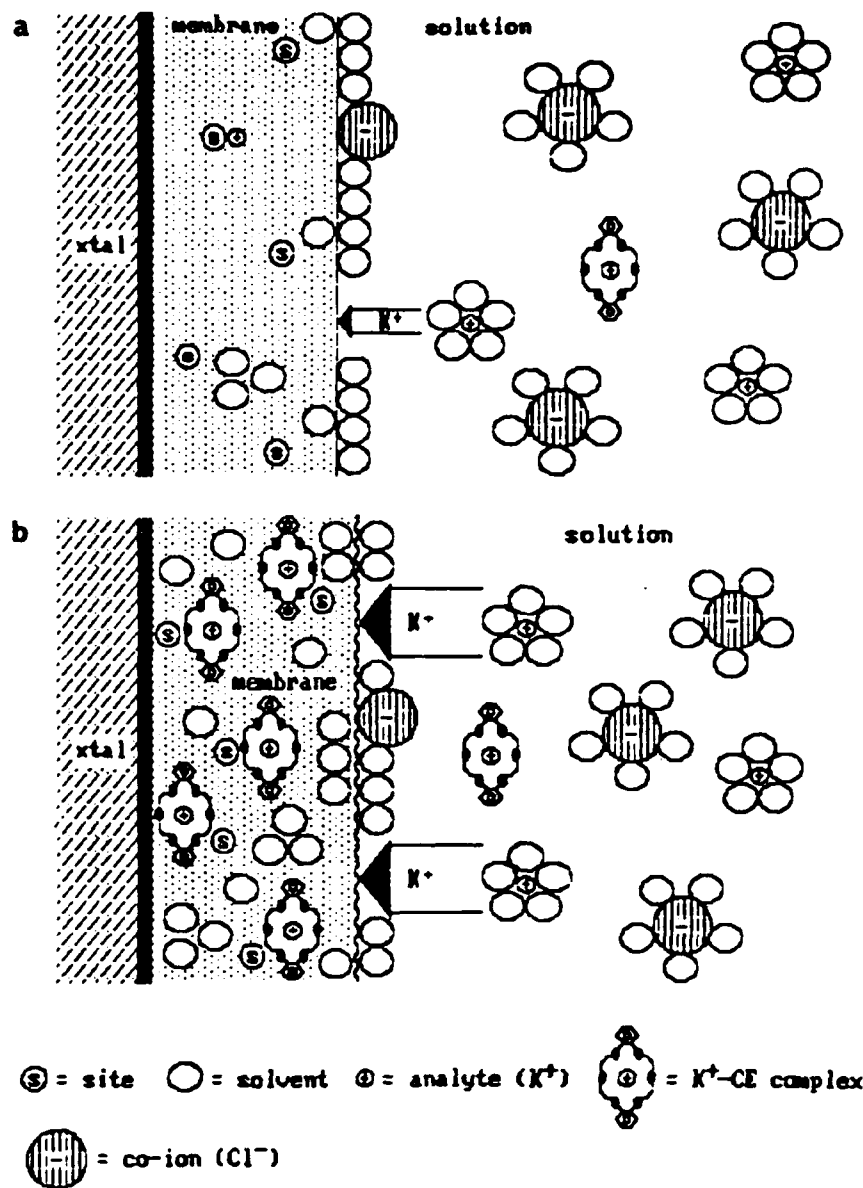


Figure 3.10 Illustration showing reference and sensor membranes' responses to analyte solutions. a. Reference membrane. Some analyte (and accompanying solvent) enters the membrane due to the ion exchange capabilities of PVC. b. Sensor membrane. A considerable amount of analyte (and accompanying solvent) enters the membrane due to the ionophore and PVC ion exchange capabilities.



Since the ionophore concentrations in the PVC ISE membranes exceed the site concentrations, Donnan failure occurs when the site concentrations are exceeded. The effects discussed above therefore make PVC a poor candidate for sensor films in QCM-based ionic sensors.

QCM-based sensors based on these membranes are impractical because of the problems associated with the thin PVC membranes (short lifetimes, response variation between sets, extensive solvent swelling, etc.). Several successful QCM-membrane sensors utilizing different polymeric matrices have been devised,<sup>35-36</sup> however. The potential for a two-dimensional analytical technique based on concurrent mass and electrochemical sensing capabilities of this type of system is feasible and could hold great promise as an analytical tool.<sup>100</sup>

## REFERENCES

1. Janata, J. *Principles of Chemical Sensors*; Plenum Press: New York, 1989.
2. Kumins, C.A.; London, A. *J. Polym. Sci.*, 1960, **66**, 395.
3. Shatkay, A. *Anal. Chem.*, 1967, **39**, 1056.
4. Moody, G.J.; Oke, R.B.; Thomas, J.D.R. *Analyst*, 1970, **95**, 910.
5. Davies, J.E.W.; Moody, G.J.; Thomas, J.D.R. *Analyst*, 1972, **97**, 87.
6. a) Griffiths, G.H.; Moody, G.J.; Thomas, J.D.R. *Analyst*, 1972, **97**, 420. b) Craggs, A.; Moody, G.J.; Thomas, J.D.R. *J. Chem. Ed.*, 1974, **51**, 541.
7. Thomas, J.D.R. *Anal. Chim. Acta*, 1986, **180**, 289.
8. Armstrong, R.D.; Covington, A.K.; Proud, W.G. *J. Electroanal. Chem.*, 1988, **257**, 155.
9. Armstrong, R.D.; Wang, H.; Todd, M. *J. Electroanal. Chem.*, 1989, **266**, 173.
10. Sears, J.K.; Darby, J.R. *The Technology of Plasticizers*; John Wiley and Sons: New York, 1982; Chapters 1,2,4-6.
11. Zhou, Z.; Xie, R.Y.; Christian, G.D. *Anal. Lett.*, 1986, **19**, 1747.

12. Ammann, D.; Morf, W.E.; Anker, P.; Meier, P.C.; Pretsch, E.; Simon, W. *Ion-Selective Electrode Rev.*, 1983, 5, 3.
13. Okada, T.; Hiratani, K.; Sugihara, H. *Analyst*, 1987, 112, 587.
14. Horvai, G.; Horvath, V.; Farkas, A.; Pungor, E. *Anal. Lett.*, 1988, 21, 2165.
15. Morf, W.E.; Simon, W.; Wuhrmann, P., *Anal. Chem.*, 1976, 48, 1031.
16. Craggs, A.; Moody, G.J.; Thomas, J.D.R.; Willcox, A., *Talanta*, 1976, 23, 799.
17. Thoma, A.P.; Viviani-Nauer, S.; Arvantis, S.; Morf, W.E.; Simon, W., *Anal. Chem.*, 1977, 49, 1567.
18. Buck, R.P.; Boles, J.H. *Anal. Chem.*, 1972, 45, 2057.
19. Lev, A.A.; Malez, V.V; Osipov, V.V In *Membranes*; Eisenman, G., Ed.; Marcel Dekker: New York, 1973; Vol. 2.
20. Kedem, O.; Bloch, R.; Perry, M., *IUPAC Intern. Symp. on Selective Ion-Sensitive Electrodes*; Cardiff: 1973; Paper 44.
21. Luch, J.R.; Higuchi, T.; Sternson, L.A., *Anal. Chem.*, 1982, 54, 1583.
22. Crawley, C.D.; Rechnitz, G.A., *J. Membr. Sci.*, 1985, 24, 201.

23. Horvai, G.; Graf, E.; Toth, K.; Pungor, E.; Buck, R.P., *Anal. Chem.*, 1986, 58, 2735.
24. Horvai, G.; Graf, E.; Toth, K.; Pungor, E.; Buck, R.P., *Anal. Chem.*, 1986, 58, 2741.
25. Horvai, G.; Graf, E.; Toth, K.; Pungor, E.; Buck, R.P., *J. Electroanal. Chem.*, 1987, 223, 51-66.
26. Pungor, E.; Iglehart, M.L.; Buck, R.P., *Anal. Chem.*, 1988, 60, 290.
27. Lindner, E.; Graf, E.; Niegriesz, Z.; Toth, K.; Pungor, E.; Buck, R.P., *Anal. Chem.*, 1988, 60, 295.
28. Horvai, G.; Pungor, E.; Iglehart, M. P.; Buck, R.P., *Anal. Chem.*, 1988, 60, 1018.
29. Morf, W.E.; Simon, W., *Anal. Lett.*, 1989, 22, 1171.
30. van der Berg, A.; van der Wal, P.D.; Skowronska-Ptasinska, M.; Sudholter, E.J.R.; Reinhoudt, D.N., *Anal. Chem.*, 1987, 59, 2827.
31. Morf, W.E.; Simon, W., *Helv. Chim. Acta*, 1986, 69, 1120 .
32. Armstrong, R.D. *Electrochimica Acta*, 1987, 32, 1549.
33. Oesch, U.; Simon, W. *Anal. Chem.*, 1980, 52, 692.
34. Hlavay, J.; Guilbault, G.G, *Anal. Chem.*, 1977, 49, 890.
35. Guilbault, G.G., *Ion-Selective Electrode Rev.*, 1980, 2, 3.

36. Lasky, S.J.; Buttry, D.A. In *Chemical Sensors and Microinstrumentation*; Murray, R.W.; Dessy, R.E.; Heineman, W.R.; Janata, J.; Seitz, W.R., Eds.; American Chemical Society: New York, 1989; ACS Symposium Series, No. 403.
37. Salt, D. *Hy-Q Handbook of Quartz Crystal Devices*; Van Nostrand Reinhold Co.: Berkshire, England, 1987.
38. Sauerbrey, G. *Z. Physik*, 1959, 155, 206.
39. Bottom, V.E. *Introduction to Quartz Crystal Unit Design*; Van Nostrand Reinhold Co.: New York, 1982.
40. Frerking, M.E. *Crystal Oscillator Design and Temperature Compensation*; Van Nostrand Reinhold Co.: New York, 1978.
41. *Applications of the Piezoelectric Quartz Crystal Microbalance. Methods and Phenomena.*; Lu, C. Czanderna, A., Eds.; Elsevier: New York, 1984; Vol. 7, Ch. 1 and 2.
42. Bahadur, P.; Parshad, R. In *Physical Acoustics*; Mason, W.P.; Thurston, R.N., Eds.; Academic Press: New York, 1982; Vol. 16, Ch. 2.
43. Ullevig, P.M.; Evans, J.F.; Albrecht, M.G. *Anal. Chem.*, 1982, 54, 2341.
44. Buttry, D.A. In *Electroanalytical Chemistry*; Bard, A.J., Ed.; Marcel Dekker: New York, 1990; Vol. 17, in press.
45. *Fundamentals of Quartz Oscillators*; Hewlett-Packard Application Note 200-2.

46. Varineau, P.T; Buttry, D.A *J. Phys. Chem.*, 1987, 91, 1292.
47. Varineau, P.T. *Ph.D. Thesis*; University of Wyoming: Laramie, Wyoming, 1989; p.28.
48. Stockbridge, C.D In *Vacuum Microbalance Techniques*; Behrndt, K.H., Ed.; Plenum: New York, 1966; Vol. 5, p. 193.
49. Miller, J.G.; Bolef, D.I. *J. Appl. Phys.*, 1968, 39, 5815.
50. Lu, C.; Lewis, O. *J. Appl. Phys.*, 1972, 43, 4395.
51. Benes, E. *J. Appl. Phys.*, 1984, 56, 608.
52. Guilbault, G.G.; Hlavay, J. *Anal. Chem.*, 1977, 49, 1890.
53. Guilbault, G.G.; Ho, M.H.; Schiede, E.P. *Anal. Chim. Acta*, 1981, 130, 141.
54. Glassford, A.P.M. *J. Vac. Sci. Technol.*, 1978, 15, 1836.
55. Nomura, T. *Anal. Chim. Acta*, 1981, 124, 81.
56. Nomura, T.; Hattori, O. *Anal. Chim. Acta*, 1980, 115, 323.
57. Konash, P.L.; Bastiaans, G.J. *Anal. Chem.*, 1980, 52, 1929.
58. Bruckenstein, S.; Shay, M. *Electrochimica Acta*, 1985, 30, 1295.

59. Hunter, R.J. *Zeta Potential in Colloid Science*; Academic Press: New York, 1981. Chapters 1 and 5.
60. Mpandou, A.; Siffert, B. *J. Coll. Interfac. Sci.*, 1984, 102, 138.
61. Kanazawa, K.K.; Gordon, J.G. *Anal. Chim. Acta*, 1985 175, 99.
62. Kanazawa, K.K.; Gordon, J.G. *Anal. Chem.*, 1985, 57, 1770.
63. Muramatsu, H.; Tamiya, E.; Karube, I. *Anal. Chem.*, 1988, 60, 2142.
64. Ferry, J.D. *Viscoelastic Properties of Polymers*; John Wiley and Sons: New York, 1980; Chapters 1 and 2.
65. Kanazawa, K.K. *IBM Technical Report #RJ 5125*; IBM Research Laboratory: San Jose, CA, 1986.
66. Reed, C.E.; Kaufman, J.F.; Kanazawa, K.K. Preprint.
67. Donohue, J.J.; Buttry, D.A. Unpublished results.
68. Schumacher, R.; Borges, G.; Kanazawa, K.K. *Surf. Sci. Lett.*, 1985, 163, L621.
69. Schumacher, R.; Gordon, J.G.; Melroy, O. J. *Electroanal. Chem.*, 1987, 216, 127.
70. Ostrom, G.S.; Buttry, D.A. *J. Electroanal. Chem.*, 1988, 256, 411.
71. Lasky, S.J.; Meyer, H.R.; Buttry, D.A. In *IEEE Technical Digest on Sensors and Actuators*; IEEE Press: New York, 1990; in press.

72. Cady, W.G. *Piezoelectricity*; McGraw-Hill: New York, 1946; Chapter 1.
73. Pulker, H.K. *Thin Solid Films*, 1976, 32, 27.
74. Strutt, J.W. (Lord Raleigh) *The Theory of Sound*; Dover: New York, 1945; Rev. Ed., p.117.
75. Kurosawa, S.; Tawara, E.; Kamo, N.; Kobatake, Y. *Anal. Chim. Acta*, 1990, 230, 41.
76. Borjas, R.; Buttry, D.A. *J. Electroanal. Chem.*, 1990, 280, 73.
77. King, W.H.; Steidler, F.E.; Vargar, G.M. *Phase I-III Report for Martin-Marietta Corp., Contract RCI-201036*; Linden N.J.: 1965.
78. Karasek, F.W.; Tiernay, J.M. *J. Chromatogr.*, 1974, 89, 31.
79. Henderson, D.E.; Taranto, M.B.; Tonkin, W.G.; Ahlgren, D.J.; Gatenby, D.A.; Woh Schum, T. *Anal. Chem.*, 1982, 54, 2067.
80. Nomura, T.; Watanabe, M.; West, T.S. *Anal. Chim. Acta*, 1985, 175, 107.
81. Karmarkar, K.H.; Guilbault, G.G. *Anal. Chim. Acta*, 1975, 75, 111.
82. Nomura, T.; Okuhara, M. *Anal. Chim. Acta*, 1982, 142, 281.



83. Guilbault, G.G.; Lubrano, G.; Ngeh, J.; Jordan, J.; Foley, P.; *Report, CRDEC-CR-87056*; NTIS: Washington, D.C., 1989.
84. Laatikainen, M.; Lindstrom, M. *J. Colloid Interfac. Sci.*, 1987, 125, 610.
85. Nordin, S.-A.; Kasemo, B. *Progr. Colloid Polym. Sci.*, 1988, 76, 51.
86. Ognjanovic, R.; Hui, C.-Y.; Kramer, E.J. *J. Mater. Sci.*, 1990, 25, 514.
87. Guilbault, G.G. *CRC Critical Reviews in Analytical Chemistry*, 1988, 17, 1.
88. Bruckenstein, S.; Shay, M. *J. Electroanal. Chem.*, 1985, 188, 131.
89. Lasky, S.J.; Buttry, D.A. *J. Am. Chem. Soc.*, 1987, 110, 6258.
90. Horvai, G.; Horvath, V.; Farkas, A.; Pungor, E. *Talanta*, 1989, 36, 403.
91. *Handbook of Organic Analytical Reagents*; Cheng, K.L., Ueno, K., Imamura, T., Eds.; CRC Press: Boca Raton, FL, 1982.
92. Armstrong, R.D.; Horvai, G. *Electrochimica Acta*, 1990, 35, 1.
93. Thomas, J.D.R. *J. Chem. Soc., Faraday Trans. 1*, 1986, 82, 1135.

94. Craggs, A.; Keil, A.; Moody, G.J.; Thomas, J.D.R.  
*Talanta*, 1976, 22, 907.
95. Attiyat, A.S.; Christian, G.D.; Hallman, J.D.; Bartsch,  
R.A. *Talanta*, 1988, 35, 769.
96. Moody, G.J.; Thomas, J.D.R.; Slater, J.M. *Analyst*, 1988,  
113, 1703.
97. Thomas, J.D.R. *Anal. Lett.*, 1989, 22, 1057.
98. Moody, G.J.; Saad, B.; Thomas, J.D.R. *Analyst*, 1989,  
114, 15.
99. Armstrong, R.D.; Johnson, B. *Corros. Sci.* In press.
100. Deakin, M.R.; Byrd, H. *Anal. Chem.*, 1989, 60, 290.
101. Moody, G.J.; Thomas, J.D.R. In *Ion-Selective Electrodes  
in Analytical Chemistry*; Freiser, H., Ed.; Plenum: New  
York, 1978.